



# UNIVERSIDAD DE INVESTIGACIÓN DE TECNOLOGÍA EXPERIMENTAL YACHAY

Escuela de Ciencias Biológicas e Ingeniería

**TÍTULO: Drug delivery system: Designing hydrogels as  
machinery for anti-inflammatory therapeutics from plant  
diversity of Ecuador.**

Trabajo de integración curricular presentado como requisito para la  
obtención del título de Ingeniera Biomédica

**Autora:**

Zamora Mendoza Lizbeth Carolina

**Tutor:**

Diego Lucero, Ph.D.

**Co-Tutor:**

Frank Alexis, Ph.D.

Nelson Vispo, Ph.D.

Urcuquí, Octubre 2022

---

**SECRETARÍA GENERAL  
ESCUELA DE CIENCIAS BIOLÓGICAS E INGENIERÍA  
CARRERA DE BIOMEDICINA  
ACTA DE DEFENSA No. UITEY-BIO-2022-00030-AD**

En la ciudad de San Miguel de Urququí, Provincia de Imbabura, a los 11 días del mes de octubre de 2022, a las 09:30 horas, en el Aula DGP103 de la Universidad de Investigación de Tecnología Experimental Yachay y ante el Tribunal Calificador, integrado por los docentes:

<b>Presidente Tribunal de Defensa</b>	Dra. SPENCER VALERO, LILIAN MARITZA , Ph.D.
<b>Miembro No Tutor</b>	Dra. LIRA VERGARA RENE CONSTANZA , Ph.D.
<b>Tutor</b>	LUCERO BORJA, DIEGO SEBASTIAN

Se presenta el(la) señor(ita) estudiante **ZAMORA MENDOZA, LIZBETH CAROLINA**, con cédula de identidad No. **1726564089**, de la **ESCUELA DE CIENCIAS BIOLÓGICAS E INGENIERÍA**, de la Carrera de **BIOMEDICINA**, aprobada por el Consejo de Educación Superior (CES), mediante Resolución **RPC-SO-43-No.496-2014**, con el objeto de rendir la sustentación de su trabajo de titulación denominado: **Drug delivery system: Designing hydrogels as machinery for anti-inflammatory therapeutics from plant diversity of Ecuador**, previa a la obtención del título de **INGENIERO/A BIOMÉDICO/A**.

El citado trabajo de titulación, fue debidamente aprobado por el(los) docente(s):

<b>Tutor</b>	LUCERO BORJA, DIEGO SEBASTIAN
<b>Co - Tutor</b>	Dr. ALEXIS FRANK , Ph.D.

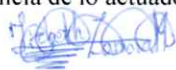
Y recibió las observaciones de los otros miembros del Tribunal Calificador, las mismas que han sido incorporadas por el(la) estudiante.

Previamente cumplidos los requisitos legales y reglamentarios, el trabajo de titulación fue sustentado por el(la) estudiante y examinado por los miembros del Tribunal Calificador. Escuchada la sustentación del trabajo de titulación, que integró la exposición de el(la) estudiante sobre el contenido de la misma y las preguntas formuladas por los miembros del Tribunal, se califica la sustentación del trabajo de titulación con las siguientes calificaciones:

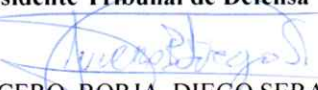
Tipo	Docente	Calificación
Presidente Tribunal De Defensa	Dra. SPENCER VALERO, LILIAN MARITZA , Ph.D.	9,3
Miembro Tribunal De Defensa	Dra. LIRA VERGARA RENE CONSTANZA , Ph.D.	9,6
Tutor	LUCERO BORJA, DIEGO SEBASTIAN	8,8

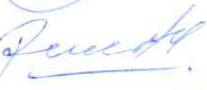
Lo que da un promedio de: **9.2 (Nueve punto Dos)**, sobre 10 (diez), equivalente a: **APROBADO**

Para constancia de lo actuado, firman los miembros del Tribunal Calificador, el/la estudiante y el/la secretario ad-hoc.

  
ZAMORA MENDOZA, LIZBETH CAROLINA  
**Estudiante**

  
Dra. SPENCER VALERO, LILIAN MARITZA , Ph.D.  
**Presidente Tribunal de Defensa**

  
LUCERO BORJA, DIEGO SEBASTIAN  
**Tutor**

  
Dra. LIRA VERGARA RENE CONSTANZA , Ph.D.  
**Miembro No Tutor**

KARLA ALARCON

**ALARCON FELIX, KARLA ESTEFANIA**  
**Secretario Ad-hoc**

# Autoría

Yo, LIZBETH CAROLINA ZAMORA MENDOZA, con cédula de identidad 1726564089, declaro que las ideas, juicios, valoraciones, interpretaciones, consultas bibliográficas, definiciones y conceptualizaciones expuestas en el presente trabajo; así cómo, los procedimientos y herramientas utilizadas en la investigación, son de absoluta responsabilidad de el/la autor/a del trabajo de integración curricular. Así mismo, me acojo a los reglamentos internos de la Universidad de Investigación de Tecnología Experimental Yachay.

Urququí, Octubre del 2022.



---

Lizbeth Zamora Mendoza

CI: 1726564089

# Dedication

This research work is the fruit of countless and arduous sacrifices. These lines are dedicated to people who serve as inspiration as brilliant scientists, good friends, and  
mentors.

To God for his blessings in our everyday lives. To my parents, Vicente and Holanda, for their infinite love, support, and commitment to my education. To my sisters, Mercedes, Cristina and Janelle, for their continuous motivation and advice. A special feeling of gratitude to my relatives, mentors and classmates for their guidance, efforts and  
encouragement.

Lizbeth Zamora Mendoza



# Acknowledgment

The path of science does not require speed; it requires perseverance, hard work, and responsibility.

I would like to acknowledge the unconditional support of my family. I am deeply grateful to my parents, Vicente and Holanda, for always motivating me to pursue my dreams and giving me the best advice and keen interest in my academic achievements. I am thankful to my sisters, Mercedes, Janelle, and Cristina, for all the support.

I am thankful to Prof. Dr. Diego Lucero for his contribution and guidance to this research project.

I thankfully acknowledge the support and inspiration of Prof. Dr. Frank Alexis for allowing me to learn about biomaterials, an area that I am passionate about, and for his for providing facilities to carry out this research work.

I am also thankful to Prof. Dr. Nelson Vispo for his comments and suggestions in this research project, for believing in my capacities from the first semester, and for introducing me to the molecular and cellular research field.

I would also like to thank my professors, technician, and classmates for their kind help and priceless suggestions.

I am also indebted to my friends (Y,P,MJ,LL,R,E,J,T,K,R,C,S,F,P,J,L,R,A), who always looked forward to making my educational career successful and becoming my Yachay Tech family.

Lizbeth Zamora Mendoza



# Resumen

Recientemente, diversas plantas medicinales han sido una fuente natural de compuestos farmacológicos. En el presente estudio, extractos vegetales (L001-M, L002-E, L003-M and L004-E) se obtuvieron mediante extracción por maceración en metanol y etanol como solvente. Los compuestos bioactivos se caracterizaron mediante screening fitoquímico para identificar sus metabolitos secundarios. Se identificó a través de FT-IR los grupos funcionales correspondientes a alcaloides, saponinas, terpenos, flavonoides, fenoles y taninos. Además, se utilizó técnicas de cromatografía de capa fina y el espectro UV/Vis para referir la diversidad de componentes en los extractos. Esta investigación también evaluó la actividad biológica de los extractos en ensayos antimicrobianos, antioxidantes y anti-inflamatorios con el fin analizar su potencial aplicación farmacéutica. La concentración mínima bactericida de las muestras L001-M y L002-E en bacteria Gram negativa *Escherichia Coli* fue a 2.5 mg/mL. La actividad antioxidante *in vitro* se evaluó mediante el ensayo del Poder Reductor Férrico y la Actividad Antioxidante Total demostrando que los extractos metanólicos (L001-M y C003-M) fueron mejores compuestos antioxidantes comparado con los extractos etanólicos (L002-E y C004-E). Además, la inhibición de la hemólisis inducida por hipotonicidad resultó positiva para L001-M, L002-E y C004-E. Los hidrogeles de celulosa de algodón (NRC) y celulosa microcristalina (MCC) formulados con los cuatro extractos se estudiaron cinética, estructural y morfológicamente. La incorporación de los extractos en los hidrogeles se verificó mediante el ensayo FT-IR, y su análisis mediante estereoscopia. Los estudios cinéticos revelaron que el tipo MCC mostró mejores valores de hinchamiento (45% a 140%) que los hidrogeles NRC (49% a 95%). También se estudiaron los perfiles de liberación de los extractos en PBS con pH 7.4 donde el tipo NRC (50%) mostró mejores resultados que el hidrogel MCC (30%). La actividad biológica eficaz de los hidrogeles en la línea celular DH5- $\alpha$  (*E. Coli*) fue registrada. Los resultados

globales sugieren la efectiva encapsulación de los extractos naturales en hidrogeles como sistemas de liberación controlada que sugiere su posible aplicación biomédica.

**Palabras Clave:** sistema de liberación de extractos, actividad antioxidante, actividad anti-inflamatoria, actividad antibacteriana, metabolitos secundarios.

# Abstract

Nowadays, several medicinal plants have been a natural source of pharmacological compounds. The present study extracted plant extracts (L001-M, L002-E, L003-M, and L004-E) by maceration in methanol and ethanol as solvents. The bioactive compounds were characterized by phytochemical screening to identify their secondary metabolites content. The functional groups corresponding to alkaloids, saponins, terpenes, flavonoids, phenols, and tannins were identified by FT-IR. In addition, thin layer chromatography techniques and UV/Vis spectra were used to analyze the components in the extracts. This research also evaluated the biological activity of the extracts in antimicrobial, antioxidant, and anti-inflammatory assays to analyze their potential pharmaceutical application. The minimum bactericidal concentration of samples L001-M and L002-E on Gram-negative bacteria *Escherichia Coli* was 2.5 mg/mL. The *in vitro* antioxidant activity was evaluated by the Ferric Reducing Power and Total Antioxidant Activity assay showing that the methanolic extracts (L001-M and C003-M) were better antioxidant compounds compared to the ethanolic extracts (L002-E and C004-E). In addition, inhibition of hypotonicity-induced hemolysis was positive for L001-M, L002-E, and C004-E. Cotton cellulose (NRC) and microcrystalline cellulose (MCC) hydrogels formulated with the four extracts were studied kinetically, structurally, and morphologically. The incorporation of the extracts into the hydrogels was verified by FT-IR assay and their analysis by stereoscope. Kinetic studies revealed that the MCC type showed better swelling values (45% to 140%) than the NRC hydrogels (49% to 95%). The release profiles of the extracts were also studied in PBS at pH 7.4, where the NRC type (50%) showed better results than the MCC hydrogel (30%). The effective biological activity of the hydrogels on the DH5- $\alpha$  cell line (*E. coli*) was recorded. The overall results suggest the effective encapsulation of the natural extracts in hydrogels as controlled release systems suggesting their possible biomedical application.

**Keywords:** Extract delivery system, antioxidant activity, anti-inflammatory activity, antibacterial activity, secondary metabolites.

# Contents

<b>Dedication</b>	<b>iii</b>
<b>Acknowledgment</b>	<b>v</b>
<b>Resumen</b>	<b>vii</b>
<b>Abstract</b>	<b>ix</b>
<b>Contents</b>	<b>xi</b>
<b>List of Tables</b>	<b>xiii</b>
<b>List of Figures</b>	<b>xv</b>
<b>1 Introduction</b>	<b>1</b>
1.1 Background . . . . .	1
1.2 Problem statement . . . . .	3
1.3 Hypothesis . . . . .	3
1.4 Objectives . . . . .	3
1.5 Justification . . . . .	4
<b>2 Theoretical Framework</b>	<b>5</b>
2.1 Phytomedicine . . . . .	5
2.2 Secondary metabolites . . . . .	5
2.3 Action mechanism of plant extracts against bacteria . . . . .	6
2.4 Action mechanism of antioxidant activity of plant extracts . . . . .	6
2.5 <i>In vitro</i> anti-inflammatory action mechanism of plant extracts . . . . .	7
2.6 Novel delivery systems loaded with bioactive plant compounds . . . . .	7

<b>3</b>	<b>Phytochemical and spectrophotometric characterization of extracts</b>	<b>9</b>
3.1	Reagents and equipment . . . . .	9
3.2	Ethanolic and methanolic extract preparation . . . . .	10
3.3	Phytochemical Screening . . . . .	11
3.4	Thin Layer Chromatography (TLC) . . . . .	15
3.5	Spectrophotometric characterization . . . . .	17
3.5.1	UV/Vis spectrum and NanoDrop analysis . . . . .	17
3.5.2	FT-IR spectrum . . . . .	21
<b>4</b>	<b>Biological activity: antibacterial, antioxidant and anti-inflammatory</b>	<b>27</b>
4.1	Reagents and equipment . . . . .	27
4.2	Antibacterial activity: Minimum Bactericidal Concentrations (MBC's) . . . . .	28
4.3	Relative Antibacterial Capacity . . . . .	31
4.4	<i>In vitro</i> antioxidant activity . . . . .	33
4.4.1	Ferric Reducing Power assay (FRP) . . . . .	33
4.4.2	Total Antioxidant Activity (TAC) by phosphomolybdenum method . . . . .	37
4.5	<i>In vitro</i> anti-inflammatory activity . . . . .	40
<b>5</b>	<b>Development of hydrogels using botanical extracts</b>	<b>45</b>
5.1	Reagents and equipment . . . . .	45
5.2	Synthesis and characterization of hydrogel . . . . .	45
5.2.1	Cellulose hydrogel synthesis . . . . .	45
5.2.2	Fourier-Transform Infrared spectroscopy . . . . .	46
5.2.3	Surface morphology of hydrogel . . . . .	48
5.3	Density and swelling of hydrogel . . . . .	50
5.4	Loaded-hydrogel release profiles . . . . .	54
5.5	Biological activity of loaded-hydrogel . . . . .	57
<b>6</b>	<b>Conclusions</b>	<b>61</b>
	<b>Bibliography</b>	<b>65</b>

# List of Tables

3.1	Ethanollic and methanollic yield of extracts . . . . .	11
3.2	Phytochemical screening of methanollic and ethanollic extracts. . . . .	14
3.3	UV-VIS profiles of secondary metabolites. . . . .	20
4.1	Antimicrobial screening test of effective extract against DH5- $\alpha$ . . . . .	29
4.2	FRAP value in AEAC (mg AA/g) and Reducing power (%RP) . . . . .	36
4.3	Total antioxidant activity of plant extracts . . . . .	40
5.1	Cellulose hydrogel density. . . . .	52
5.2	Maximum peak based on UV-Vis spectra of plants extracts . . . . .	55
5.3	Antibacterial activity of extract loaded-hydrogel, NA = non active . . . . .	58



# List of Figures

3.1	Maceration procedure to obtain the plant extracts . . . . .	10
3.2	UV-light lamp 365 nm (blue plate) and the sulfuric acid/vainillina (cream plate) revealing of extract. . . . .	16
	(a) L001-M . . . . .	16
	(b) L002-E . . . . .	16
3.3	UV-light lamp 365 nm (blue plate) and the sulfuric acid/vainillina (cream plate) revealing of extract. . . . .	17
	(a) C003-M . . . . .	17
	(b) C004-E . . . . .	17
3.4	UV-VIS spectra of extract samples . . . . .	19
	(a) L001-M . . . . .	19
	(b) L002-E . . . . .	19
	(c) C003-M . . . . .	19
	(d) C004-E . . . . .	19
3.5	NanoDrop spectra of extract samples . . . . .	21
	(a) L001-M . . . . .	21
	(b) L002-E . . . . .	21
	(c) C003-M . . . . .	21
	(d) C004-E . . . . .	21
3.6	FT-IR of plant extracts . . . . .	22
	(a) L001-M . . . . .	22
	(b) L002-E . . . . .	22
3.7	FT-IR spectra of extract samples . . . . .	24

(a)	C003-M . . . . .	24
(b)	C004-E . . . . .	24
4.1	Antibacterial activity of the plant extract. . . . .	29
(a)	L001-M in DH5 . . . . .	29
(b)	L001-M in E410A5 . . . . .	29
(c)	L001-M in TG1 . . . . .	29
(d)	L002-E in DH5 . . . . .	29
(e)	L002-E in E410A5 . . . . .	29
(f)	L002-E in TG1 . . . . .	29
4.2	Antibacterial activity of the plant extract. . . . .	30
(a)	C003-M in DH5 . . . . .	30
(b)	C003-M in E410A5 . . . . .	30
(c)	C003-M in TG1 . . . . .	30
(d)	C004-E in DH5 . . . . .	30
(e)	C004-E in E410A5 . . . . .	30
(f)	C004-E in TG1 . . . . .	30
4.3	Bacterial growth curves formed from OD600 measurements of extracts . . .	32
(a)	L001-M . . . . .	32
(b)	L002-E . . . . .	32
4.4	Ferric reducing power assay procedure . . . . .	34
4.5	The absorbance of plant extract in Ferric Reducing Power determination. .	35
(a)	L001-M . . . . .	35
(b)	L002-E . . . . .	35
(c)	C003-M . . . . .	35
(d)	C004-E . . . . .	35
4.6	Ferric Reducing Power assay procedure . . . . .	36
4.7	Ferric Reducing Power results comparison of plant extract and standard . .	37
(a)	L001-M, L002-E and Ascorbic Acid . . . . .	37
(b)	C003-M, C004-E and Ascorbic Acid . . . . .	37
4.8	Total antioxidant activity by phosphomolybdenum method . . . . .	38

4.9	Total antioxidant activity of plant extracts . . . . .	39
(a)	L001-M . . . . .	39
(b)	L002-E . . . . .	39
(c)	C003-M . . . . .	39
(d)	C004-E . . . . .	39
4.10	Anti-inflammatory activity of the plant extract comparing its effectiveness with the commercial Aspirin. . . . .	42
4.11	Anti-inflammatory activity of the plant extract comparing its effectiveness with the commercial Aspirin. . . . .	42
5.1	Synthesis of cellulose hydrogel with plants extracts . . . . .	46
5.2	Extract loaded-hydrogels relative structure. . . . .	46
5.3	FT-IR Spectrum of plant extract (green line=spectrum with extract) com- pared with WE hydrogels (red line=spectrum without extract). . . . .	47
(a)	L001-M/NRC . . . . .	47
(b)	L001-M/MCC . . . . .	47
(c)	L002-E/NRC . . . . .	47
(d)	L002-E/MCC . . . . .	47
5.4	FT-IR Spectrum of plant extract (green line=spectrum with extract) com- pared with WE hydrogels (red line=spectrum without extract). . . . .	48
(a)	C003-M/NRC . . . . .	48
(b)	C003-M/MCC . . . . .	48
(c)	C004-E/NRC . . . . .	48
(d)	C004-E/MCC . . . . .	48
5.5	Surface morphology of plant extract loaded-hydrogel through stereoscope .	49
(a)	L001-M/NRC (M=1.25) . . . . .	49
(b)	L001-M/NRC (M=4) . . . . .	49
(c)	L001-M/MCC (M=1.25) . . . . .	49
(d)	L001-M/MCC (M=4) . . . . .	49
(e)	L002-E/NRC (M=1.25) . . . . .	49
(f)	L002-E/NRC (M=4) . . . . .	49

(g)	L002-E/MCC (M=1.25) . . . . .	49
(h)	L002-E/MCC (M=4) . . . . .	49
5.6	Surface morphology of plant extract loaded-hydrogel through stereoscope .	50
(a)	C003-M/NRC (M=1.25) . . . . .	50
(b)	C003-M/NRC (M=4) . . . . .	50
(c)	C003-M/MCC (M=1.25) . . . . .	50
(d)	C003-M/MCC (M=4) . . . . .	50
(e)	C004-E/NRC (M=1.25) . . . . .	50
(f)	C004-E/NRC (M=4) . . . . .	50
(g)	C004-E/MCC (M=1.25) . . . . .	50
(h)	C004-E/MCC (M=4) . . . . .	50
5.7	Surface morphology of plant extract through stereoscope . . . . .	51
(a)	WE/NRC (M=1.25) . . . . .	51
(b)	WE/NRC (M=4) . . . . .	51
(c)	WE/MCC (M=1.25) . . . . .	51
(d)	WE/MCC (M=4) . . . . .	51
5.8	Degree of swelling of NRC and MCC hydrogels type in PBS solution. . . .	53
(a)	NRC hydrogel at 1 mg/mL . . . . .	53
(b)	NRC hydrogel at 2.5 mg/mL . . . . .	53
(c)	MCC hydrogel at 1 mg/mL . . . . .	53
(d)	MCC hydrogel at 2.5 mg/mL . . . . .	53
5.9	Plant extracts releasing data from the NRC and MCC loaded-hydrogel in PBS pH (7.4) . . . . .	56
(a)	L001-M/NRC hydrogel delivery . . . . .	56
(b)	L001-M/MCC hydrogel delivery . . . . .	56
(c)	L002-E/NRC hydrogel delivery . . . . .	56
(d)	L002-E/MCC hydrogel delivery . . . . .	56
5.10	Plant extracts releasing data from the NRC and MCC loaded-hydrogel in PBS pH (7.4) . . . . .	57
(a)	C003-M/NRC hydrogel delivery . . . . .	57
(b)	C003-M/MCC hydrogel delivery . . . . .	57

---

(c)	C004-E/NRC hydrogel delivery . . . . .	57
(d)	C004-E/MCC hydrogel delivery . . . . .	57
5.11	Antibacterial activity of the extract-loaded hydrogels. . . . .	59
(a)	L001-M/NRC and L001-M/MCC . . . . .	59
(b)	L002-E/NRC and L002-E/MCC . . . . .	59
(c)	WE/NRC and WE/MCC . . . . .	59



# Chapter 1

## Introduction

### 1.1 Background

The inflammatory phoneme and the oxidative estres are linked physiologically to several inflammatory disorders such as rheumatoid arthritis, autoimmune diseases, cancer, diabetes, and other diseases. The disorders affect millions of patients around the world. Also, the inflammatory process results after damaged tissue, in which infectious agents activate the immune system defense. The symptoms of an inflammatory process are pain, heat, redness, swelling, and loss of function [1].

Several synthetic anti-inflammatory drugs are available commercially, but their high cost and side effects can produce complications associated with the disease. Steroidal and nonsteroidal is the classification of anti-inflammatory drugs; even though they have efficient activity, side effects that affect the patients, limiting their use. Side effects include damage to the gastrointestinal fluid, liquid retention, increased blood pressure, and other symptoms like dizziness and headaches[1].

Some medicinal plants of Ecuador have been used for anti-inflammatory applications to treat affections to the population as traditional medicine. For this reason, plant-derived drugs have been studied for their potential application as a source of new drug products due to the large variety of species and the identification of unknown metabolites secondary with anti-inflammatory, antioxidant, and antibacterial therapeutic properties [2].

The ethnobotanical effects conferred by human history are linked to the toxic effects of pure chemicals. To increase the bioavailability of drugs with anti-inflammatory, antioxi-

dant, and antibacterial activity, the use of a polymeric system for controlled extract release can be used. Hydrogels are three-dimensional polymeric with crosslinked structures with the capacity to absorb water [3]. Hydrogels can be obtained from natural or synthetic polymers. Natural polymers such as chitosan, starch, and cellulose have advantages of biocompatibility, mechanical properties, density, and swelling degree. Also, cellulose hydrogels have been successfully implemented as a drug delivery system and tissue engineering.

This investigation was focused on studying two plants whose medicinal application in Ecuador corresponds to anti-inflammatory and antiseptic in the community. Literature reports indicate that plants still represent an important pool for the discovery of novel drugs and therapeutic compounds [4, 5]. Overall, the chemical characterization to identify the molecules that have therapeutic properties and performance, some *in vitro* antioxidant, anti-inflammatory, and antibacterial essays. The main objective is to search for alternatives for plant extracts application inside of polymeric biomaterials such as cellulose hydrogels to increase pharmaceutical applications.

This research project presents the synthesis and characterization of two plant extracts. It uses hydrogels as machinery for delivering anti-inflammatory, antioxidant, and antibacterial therapeutics from the plant diversity of Ecuador. Different solvents was used for extraction, and their incidence on the compounds obtained will be studied by identifying secondary metabolites such as phenols, polyphenols, steroids, and others with phytochemical tests. In addition, a chemical analysis of the extracts will be performed through UV-VIS spectrum, FT-IR spectroscopy, HPLC analysis, and Thin Layer Chromatography. Indeed, three different *in vitro* antioxidant activity assays, the application of a standardized protocol for anti-inflammatory activity, and two antibacterial studies, quantitative and qualitative, respectively, will also be performed. Finally, for the hydrogel design, the mechanical, chemical, and biological properties of the cellulose hydrogels loaded with the extracts will be studied by studying the density, swelling, release, and wear of the cellulose hydrogels.

## 1.2 Problem statement

Ecuador's medicinal plants have been used with therapeutic effects due to their high bioactive content. These plants have been used in inflammation, fever, and pain. However, there is no data available about the identification of bioactive molecules such as flavonoids, alkaloids, steroids, and other secondary metabolites [3]. This type of biomolecules would confer anti-inflammatory and antioxidant performance, and their identification in the plant extracts is critical.

Anti-inflammatory and antioxidant activity has been reported in several plants by the natural compounds characterized by polyphenolic structure and synergy with other metabolites. For this reason, medicinal plants are studied for therapeutic purposes in medicine and the application of drug delivery systems to encapsulate the bioactive compound. The current challenge is to find the optimal encapsulation method with the following characteristics: low-cost, excellent delivery performance, and easy fabrication [3]. Furthermore, hydrogels have been reported to have excellent performance and easy fabrication for biomedical applications [3]. Therefore, it is necessary to identify hydrogels' biocompatibility and mechanical properties and the correct polymer, plant extract concentration, and chemical composition valid for the plant extracts analyzed in this research.

## 1.3 Hypothesis

To investigate whether bioactive compounds from Ecuadorian plants with anti-inflammatory, antioxidant and antibacterial properties can be identified and encapsulated in polymeric hydrogel matrices.

## 1.4 Objectives

### General Objective

The present research aims to obtain chemical profiling and biological properties from two plant extract from Ecuador to design and synthesize hydrogels as machinery for the controlled delivery of antibacterial, antioxidant, and anti-inflammatory therapeutics.

### Specific Objective

To perform two ethanolic and methanolic plant extraction using the maceration method and conduct the phytochemical screening.

To characterize the secondary metabolites of several extract plants from Ecuador to understand the bio-active compounds.

To analyze the *in vitro* antioxidant and anti-inflammatory properties of several extract plants from Ecuador.

To study the qualitative and quantitative antimicrobial activity of plants through *in vitro* essays.

To design hydrogels mixed with the active compounds of several extract plants from Ecuador.

To characterize the extract-loaded hydrogel's hydrogel morphology, density, and swelling degree.

To analyze the kinetics properties of swelling and release process of the active compounds in the hydrogel and other mechanical studies.

To evaluate the biological activity of loaded hydrogel by antibacterial *in vitro* assay.

## 1.5 Justification

Before selecting the medicinal plants of Ecuador, population analysis of their use and therapeutic application was carried out. It allows firsthand empirical knowledge of the extracts and their medicinal use linked to the Ecuadorian community. Knowing that plant extracts are a precursor for discovering active biomolecules later used to generate new drugs. For this purpose, chemical analysis tools are required to take advantage of the small molecules produced by the plant to defend themselves that are recognized as secondary metabolites and obtain plant extract. Therefore, it is intended to evaluate with *in vitro* assays the antioxidant, anti-inflammatory, and antibacterial activity of the secondary metabolites present after their identification and characterization.

Thus, this work seeks to enhance the potential therapeutic use of the medicinal plant-based natural compounds studied through an encapsulation method to achieve easy administration, low production cost, and controlled release.

# Chapter 2

## Theoretical Framework

### 2.1 Phytomedicine

Drugs whose active ingredient is a plant extract elaborated by traditional pharmaceutical forms and presenting a proven biological activity. In other words, a phytomedicament is a standardized, normalized, and stabilized plant extract that offers a defined, known, and quantified pharmacological action [6].

### 2.2 Secondary metabolites

Secondary metabolites of plants are produced for essential cellular functions, metabolic pathways, and various physiological processes [7]. These metabolites protect the plant from microorganisms, infectious agents, and pathogens that affect growth and development and are responsible for each plant's color, odor, and flavor characteristics [8, 9]. Elicitors are the defensive compounds of plants against microorganisms, pests, and environmental factors. Specific secondary metabolites identified in plants were used for several pharmaceutical industry studies. They generate their immunity for the potential suppression of pathogens [10]. Polyphenols and flavonoids are phenolics compounds within the group of secondary metabolites with antioxidant and anti-inflammatory properties in medicine [11]. In addition, alkaloids and polyphenols have been identified as the possible responses for the antibacterial activity as the main components for antibiotics [12].

## 2.3 Action mechanism of plant extracts against bacteria

Plants produce antibacterial molecules to protect against predation of herbivores, insects and microorganism [13]. The antibacterial activity of a molecule occurs by chemical interference of the bacterial components, and by bypassing conventional antibacterial resistance mechanisms [14]. For example, Gonelimali et al. [15] report that plant extracts modify the microbial cell cytoplasmic pH of cells (Gram-positive and Gram-negative bacteria) by decreasing their value as well as cell membrane hyperpolarization. Kot et al. [16] also describe a bactericidal activity by p-CA hydroxycinnamic acid. It increases the plasma membrane permeability and processes related to DNA disruption. A phenolic acid such as CA shows high nucleophilic properties. Otherwise, ketone, aldehydes, ethers, and alcohols show high antibacterial activity.

## 2.4 Action mechanism of antioxidant activity of plant extracts

The plant produces antioxidant molecules for protection from ultraviolet light from the sun and reactive oxygen species during the photosynthesis process [17]. Oxidative stress is related to pathologies such as cancer, cardiac, neuronal problems, and aging because free radicals may interact with DNA, proteins, lipids, or carbohydrates [18]. Therefore, several investigations aim to identify the antioxidant activity of various plant extracts based on techniques of estimation of lipoprotein oxidation or the counting of free radicals scavenged [19]. Specifically, the exogenous antioxidants are characterized by secondary metabolites such as low molecular weight antioxidants (phenolic acids, flavonoids, carotenoids) or high molecular weight antioxidants (tannins) [20]. The reduction-oxidant reaction can be recorded, for example, with the ferric-reducing antioxidant power method by measuring the single electron transfer using reference antioxidants like gallic acid or ascorbic acid [21]. Total phenolic content assay by Folin-Ciocalteu reagent is related to non-enzyme assays, and also a single electron transfer mechanism and depends on phenolic compounds into alkaline medium depending on phenolic concentration compounds[22].

## 2.5 *In vitro* anti-inflammatory action mechanism of plant extracts

Secondary metabolites protect the plant from biotic stresses, maintain healthy growth or warn of deciduous behavior [7]. Although the inflammatory process is considered a defense mechanism for humans, it can generate serious diseases such as cancer, diabetes, y cardiovascular diseases if the inflammation process is not controlled. Some secondary metabolites belonging to the phenol, flavonoid, steroid, and glycoside groups are related to antiinflammatory activity [23]. Specifically, polyphenolic compounds from plant-based extract are of pharmacological interest by the modulation action of inflammasomes [24]. For instance, Ayertey et al. demonstrated that flavonoids minimize specific mediators of the inflammatory process such as histamine and decrease specific cytokines ( $TNF - \alpha$ ) and free radicals. Meanwhile, Fylaktaktakidou et al. [25] argue that coumarins reduce tissue bulge by stimulating decreased edema and affecting lymphoedema. Also, coumarins increase the activation of macrophages and proteolysis by lysosomal enzymes.

## 2.6 Novel delivery systems loaded with bioactive plant compounds

Nowadays, secondary metabolites with anticancer, antibacterial, anti-inflammatory and/or antioxidant activity can be obtained from extracts, essential oils, and other natural resources [26]. Nevertheless, environmental factors, pH, and metal ions in the process directly affect the chemical preservation of the molecules besides their degradation. On the other hand, pharmaceutical applications of the compounds may be limited by low bioavailability, solubility, and high volatility [27]. In particular, the molecular structures of the bioactive compounds, such as molecular weight or charge, affect the internalization by the cell, decreasing their therapeutic effects. One strategy for bioactive herbal medicine is to use a carrier for a controlled and specific release of the compounds. Various materials such as nanoparticles, lipids, or hydrogels have been developed as drug delivery systems [28].



# Chapter 3

## Phytochemical and spectrophotometric characterization of extracts

### 3.1 Reagents and equipment

The reagents used for extract synthesis and characterization correspond to methanol ( $\geq 99\%$ , Merck), ethanol ( $\geq 96\%$ , Merck), chloroform (99,8%, Merck), hydrochloric acid (37%, Merck), sodium chloride (99,9%, Merck), sulphuric acid (95-97%, Merck), ammonia solution (25%, Merck), sodium hydroxide ( $\geq 98\%$ , Sigma-Aldrich), dimethyl sulfoxide ( $\geq 99\%$ , Sigma-Aldrich), sodium carbonate (99,8%, Thermo Scientific), ferric chloride (98%, Sigma-Aldrich), and Benedict's reagent (SCIENCE Company). Previously preparing the solution of Dragendorff's and Mayer reagents were obtained from Chemical Science and Engineering School.

The analysis and characterization equipment used was: Cycle type rotor mill R-TE-651/2 (TECNAL, Brasil), Nanodrop 2000 Spectrophotometer (Thermo Scientific, USA), Cary 630 Fourier Transform Infrared Spectroscopy Spectrometer (Agilent, USA), UV/Vis/NIR Spectrophotometer Lambda 1050 (PerkinElmer, USA)

## 3.2 Ethanolic and methanolic extract preparation

The code used to identify the plant's extracts of Type 1 is L001-L002 and for Type 2 is C003-C004. The code corresponds to methanolic (M) and ethanolic (E) for solvent identification. The L001-M and L002-E correspond to plant 1, such as C003-M and C004-E to plant 2.

The two plants were collected in the Ibarra-Ecuador's flowering market. First, it was sun-dried for one day, and an oven-drying chamber was used for 24 hours. Then, it was pulverized in the shredding machine until it obtained 1-5 mm particles (See Figure 3.1.).

The extraction procedure was the maceration method. First, a determined mass of the pulverized plants was placed inside a 500 mL beaker. Then, a certain amount of solvent was added to the beaker, and the mixture was put to macerate for 15 days at room temperature. The mixture was filtered. Subsequently, the filtrates were rotoevaporated until concentrate the plant extract was. The samples were stored at 4 °C protected from sunlight until used for chemical analysis.

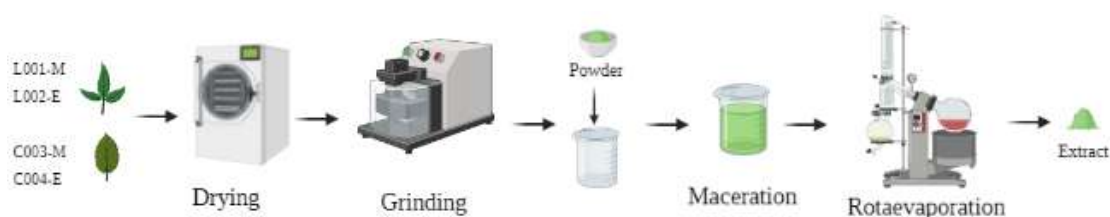


Figure 3.1: Maceration procedure to obtain the plant extracts

### Yield of extraction procedure

The extract yield was calculated with the formula (1) [29]:

$$Yield(g/100g) = \frac{(W_1 * 100)}{(W_2)} \quad (1)$$

$W_1$  is the weight of dry extract and  $W_2$  is the weight of the dry plant extract.

### Results and discussion

A strong smell and green color are obtained from C003-M and C004-E extract samples. In contrast, brown color and faint odor in the L001-M and L002-E samples. Higher yields are reported in the methanol extractions. Ethanolic and methanolic extracts yield were obtained from 5,58 % to 8,97 % (See Figure 3.1). The methanolic extract showed a higher

yield than the ethanol extracts in both plants. Additionally, the L001-M and L002-E extracts had a high yield compared to the other plant samples.

Sample	Dry plant (g)	Solvent (mL)	Dry extract (g)	Yield (%)
L001-M	15.51	150	1.3926	8.97
L002-E	14.98	150	0.9540	6.37
C003-M	15.25	150	1.0860	7.12
C004-E	15.09	150	0.4221	5.58

Table 3.1: Ethanolic and methanolic yield of extracts

### 3.3 Phytochemical Screening

The methanolic and ethanolic extracts of phytochemical compounds were analyzed by several methods to standardize the reported procedure in [30, 31, 32, 33, 34] with slight modifications to secondary metabolites identification. All the experiments were carried out in the fume extraction cabinet.

#### 1. Quaternary alkaloids and/or free amino acids

- (a) Mayer's test: In the beginning, it was prepared 1 mL of acid extract (5 mg of extract diluted in 1.50 mL of 1% hydrochloric acid). Then it was shaken and filtrated. Also, 300 uL of Mayer's solution was then filtrated. Positive result: cream-colored [30].
- (b) Dragendorff's test: The three drops of Dragendorff's reagent were added to 1 mL of acidic extract (5 mg of extract diluted in 1.50 mL of 1% hydrochloric acid). Positive reaction: orange or red precipitation [30].
- (c) Wagner's test: 300 uL of the Wagner solution was added to the filtrate of the acid extract (5 mg of extract diluted in 1.50 mL of 1% hydrochloric acid). Positive result: brown colour [30].

#### 2. Coumarins and Lactones

- Sodium hydroxide was added to the extract until yellow color appeared indicated the presence of coumarins [31].

### 3. Saponins (Frothing Test)

- One aliquot of the methanolic and ethanolic extract was diluted five times, respecting the volume of water. Then, it was stirred for 5 to 10 minutes. If there is a layer of two centimeters of foam for two minutes, the saponins test is positive [31].

### 4. Terpenes and steroids (Liebermann-Burchard Test)

- Evaporate the alcohol in a water bath; then, the extract was dissolved in 1 mL of chloroform. Then, 1 mL of anhydride acetic and 2-3 drops of concentrated sulfuric acid are added until a color change occurs to deep green color for positive result [32].

### 5. Terpenoids (Salkowski Test)

- Two mL of chloroform were added to one mL of the ethanolic and methanolic extract. Then, 0.5 mL of concentrated sulfuric acid was added drop by drop and heated for two minutes until the color changed (distinct and clear colors) depending of cholesterol reaction [32].

### 6. Reducing Sugars (Fehling Test)

- The solvent was evaporated from the extract with a water bath; the extract was diluted in 2 mL of water. Therefore, 2 mL of Fehling reactive was added and heated in water bath for 5-10 minutes. The formation of a reddish-brown colour precipitate show a content of reducing sugars [32].

### 7. Flavonoids

- (a) Alkaline reagent test: The extract was diluted in an aqueous solution and added 10% ammonium hydroxide to the solution until yellow fluorescence color occurred.
- (b) Shinoda test: The extract was diluted on 1 mL of concentrated hydrochloric acid and magnesium tape. After 5 minutes, 1 mL of amyl alcohol was added,

and the two phases were mixed and waited until they separated from red to pink color for positive result [32].

#### 8. Quinones

- (a) Borntrager test: The solvent was evaporated in a water bath, and the residue was dissolved in 1 mL of chloroform. Add 1 mL of 5% ammonium. The two phases were stirred and then waited until separated with a changed color reaction. Occurrence of red color in alkaline phase for quinones.
- (b) Acid-base test: Two drops of concentrated hydrochloric acid were added to the extract. Then, zinc powder and two drops of sodium hydroxide at 40% in another tube. The orange color indicates the presence of quinones [33].

#### 9. Phenols and tannins (Ferric chloride test)

- Three drops of 5% ferric chloride in physiological saline solution (sodium chloride at 0,9%) were added to the alcoholic extract and a positive result is a blackish precipitate [34].

#### 10. Glycosides test

- The 50 mg of extract was added to the concentrated hydrochloric acid for two hours in a water bath. Then, it was filtrated, added chloroform, and shook until the chloroform layer separated, thus ammonia solution. The pink color indicate the presence of glycosides [32].

#### 11. Mucilages (Mucilages test)

- One aliquot of the extract gets cold to 0-5 °C, and if the solution becomes gelatinous consistency is mucilage positive result [34].

#### 12. Carbohydrates (Benedict test)

- 1 mL of Benedict reagent was added to the 2 mL of extract. If green/yellow appears the amount of carbohydrates is low and red if it is high content [32].

## Results and discussion

The secondary metabolites were identified by applying several reagents to the alcoholics. The phytochemical screening of L001-M, L002-E, C003-M, and C004-E (See Table 3.2.) was applied. The L001-M extract has a high concentration of quaternary alkaloids, saponins, terpenoids, and phenols; the compounds have a high pharmacological interest. On the other hand, sample L002-E has a high content of amino acids by the Dragendorff test and saponins, steroids, terpenoids, quinones, and phenols. In the final analysis between L001-M and L002-E, although these are similar plants, it can be said that the solvent influences the secondary metabolites obtained in the extract.

Secondary Metabolite	Performed Test	L001-M	L002-E	C003-M	C004-E
Quaternary alkaloids and / or free amino acids.	Mayer Test	++	+	+++	+++
	Dragendorff Test	+++	++	+	+
	Wagner Test	++	+	++	++
Coumarins and Lactones	Coumarins and Lactones Test	+	+	+	-
Saponins	Frothing Test	+++	+++	+	+
Terpenes and steroids	Libermann-Buchard Test	+	++	+	+
Terpenoids	Salkowski Test	+++	+++	+	+
Flavonoids	Alkaline Reagent Test	+	+	+	+
	Shinoda Test	+	+	++	++
Quinones	Borntrager Test	-	+++	-	-
	Acid-base Test	-	+	+	-
Phenols and Tannins	Ferric chloride Test	+++	++	++	++
Glycosides	Test	-	+	-	+
Mucilages	Mucilages Test	-	-	-	-
Carbohydrates	Benedict Test	+	+	++	-

(+) means the presence of the secondary metabolite

(-) means the absence of the secondary metabolite

Table 3.2: Phytochemical screening of methanolic and ethanolic extracts.

In comparison, extracts C003-M and C004-E reflect a similar composition of secondary metabolites with a high content of quaternary alkaloids and free amino acids, as well as flavonoids with the Shinoda test, as well as phenols and tannins with the ferric chloride test. Indeed, the four extracts also show a lower proportion of coumarins, lactones, and carbohydrates. Phenolic compounds, such as flavonoids, are well-known as antioxidants and many other important bioactive agents [35]. According to Babbar *et al.* [36], if

secondary metabolites such as phenols and flavonoids are required, methanol is a suitable solvent. For this reason, the phytochemical screening shows polar compounds such as polyphenols and flavonoids when methanol is the solvent in contrast with ethanol.

### Extracts solubility

The L001-M and L002-E extracts were poorly soluble in water. For this reason, extracts were diluted at 1% dimethyl sulfoxide (DMSO). On the other hand, C003-M and C004-E extracts were entirely soluble in distilled water.

## 3.4 Thin Layer Chromatography (TLC)

The four plant extracts were used for the thin-layer chromatography assay. In TLC, pre-coated plates (silica gel 60F254) were applied 2-3 uL of the concentrated extract with a capillary tube. Plates were marked about 1 cm with a pencil on the bottom side and waited until  $\frac{3}{4}$  parts of the solvent covered the plates. The TLC was carried out in a chromatographic tank using the solvents systems as chloroform/acetone/formic acid (7.5:1.65:0.85) [37]. After drying, the TLC plate was revealed by a UV-light lamp (365 nm) and sulfuric acid/vainillina chemical developer.

The Retention factor (Rf) values were calculated with the equation (2) [38]:

$$Rf = \frac{\text{Distance traveled by the solvent system}}{\text{Distance traveled by the sample}} \quad (2)$$

then results were obtained.

### Results and discussion

The thin layer chromatography of L001-M, L002-E, C003-M, and C004-E extracts was applied in the silica gel 60F<sub>254</sub> for 30 minutes to separate extremely non-polar substances and analyze particular polar substances. This result shows a first approximation of the extract analyzed by extraction method and extracts content. The solvent used is chloroform/acetone/formic acid (7.5:1.65:0.85) [39].

The Rf corresponding to L001-M and L002-E is the same plant with different solvents in the extraction process (See Figure 3.2.). It could affect the secondary metabolite content in the samples. As expected, the TLC in the figure showed several Rf values that pointed out the solvent was useful. As a result, the methanolic showed more compound separation

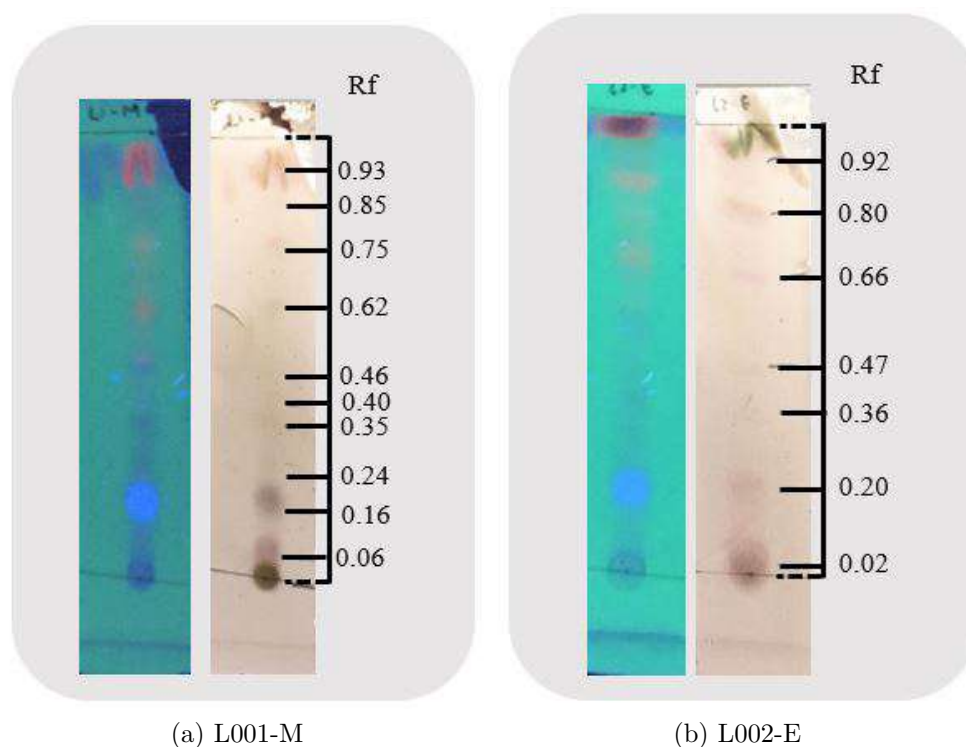


Figure 3.2: UV-light lamp 365 nm (blue plate) and the sulfuric acid/vainillina (cream plate) revealing of extract.

based on polarity than ethanolic extracts. It was registered that 0.06 in L001-M and Rf 0.02 in L002-E correspond to the same compound. Meanwhile, the Rf 0.16 and Rf 0.24 value in L001-M correspond to the Rf 0.20 compound in L002-E when sulfuric acid/vainillina revealing. Also, it was identified that a high concentration of compounds was exhibited at 0.16 and 0.20 in L001-M and L002-E, respectively, when using a UV-light lamp (365 nm).

As discussed above, the TLC of the methanolic extract reflects a major mixture of chemical components than the ethanolic extraction [40]. Using the ultraviolet light lamp at 365 nm in L001-M, the outstanding chemical compound of the extracts was obtained at Rf 0.16, while in L002-E, was at 0.20 Rf value. Also, it was identified a compound at Rf 0.95 in C003-M with UV-light lamp 365 nm revealing which is not present in the C004-E extract (See Figure 3.3.). The Rf values in both extracts describe the same compounds except in (Rf 0.47, Rf 0.55, Rf 0.97) in the C003-M extract compared to C004-E. The sulfuric acid/vanillin chromogenic reagents allow the appearance of a large number of chromatographic bands. Eventually, some chemical components were visualized only under the use of a UV-light lamp (365 nm). In figure 3.2. and 3.3. observing the region

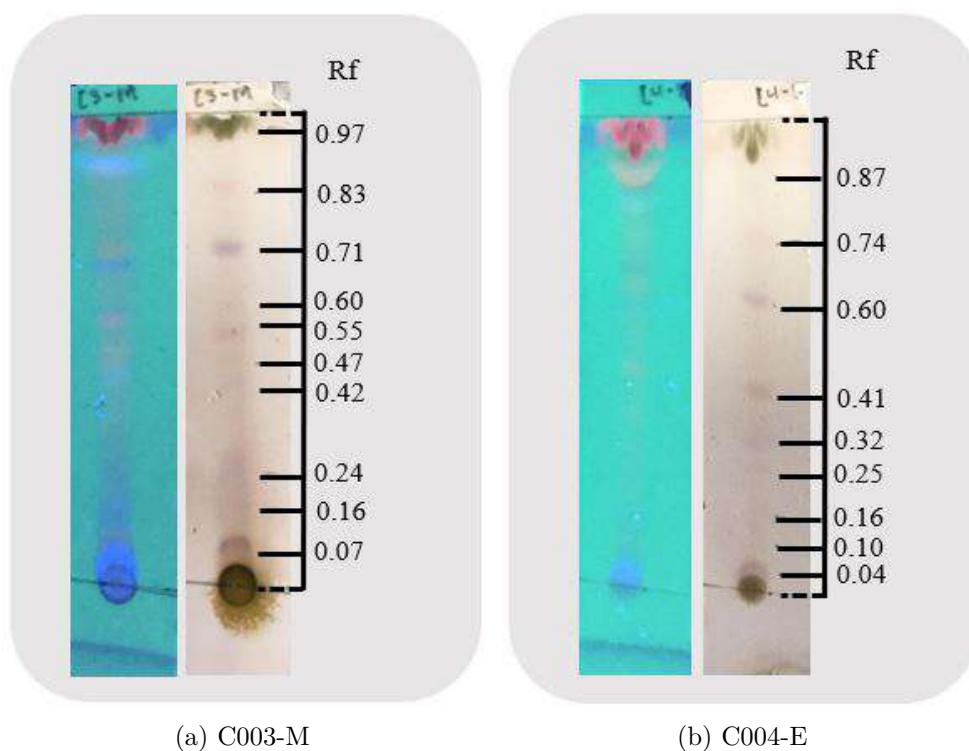


Figure 3.3: UV-light lamp 365 nm (blue plate) and the sulfuric acid/vainillina (cream plate) revealing of extract.

corresponding to the range  $R_f \geq 0.95\%$  belongs to the "impurity front" since it is the location of the impurities or compounds that, due to their polarity, are not retained previously [38]. To conclude, the TLC for L001-M, L002E, C003-M, and C004-E provides a rapid separation compound that indicates the nature of the plant extract components, which are subsequently characterized by UV-VIS spectrum and FT-IR.

## 3.5 Spectrophotometric characterization

### 3.5.1 UV/Vis spectrum and NanoDrop analysis

UV/Vis/NIR Spectrophotometer Lambda 1050 aims to analyze the phytoconstituent's presence in the L001-M, L002-E, C003-M, and C004-E samples. The UV/VIS spectrum of the plant extracts allows the identification of the profile by scanning samples in the Visible UV-visible region to obtain the characteristic peaks [41]. For the UV/Vis spectrum, the dried extracts were diluted in different concentrations to obtain the pick of the curve where there is significant absorbance. The corresponding amount of the extract was diluted

in distilled water to obtain the 0.10, 0.25, 0.50, and 1.00 mg/mL concentrations. The absorbance was measured with a quartz cell at room temperature. The wavelength range used for chemical analysis was from 250 nm to 800 nm.

Correspondingly, samples were analyzed with the Nanodrop 2000 Spectrophotometer, where a new method with the parameters of absorbance range of 190 - 340 nm and the concentration of the bioactive compounds was obtained. Extract at 1mg/mL were prepared and measured to corroborate the UV/Vis spectrum of the plant extractions performed and as a control of the profile of the samples. Therefore, the nanodrop used in the extracts allowed to quickly identify the extracts' UV-Vis profile during the preparation of total extract concentrations for the other assays and accessible verification of the components after each extraction.

## **Results and discussion**

### **UV-Vis spectra of extracts**

The UV-Vis spectra obtained showed the presence of phytoconstituents in methanolic and ethanolic extracts in the 250 - 800 nm range. The raw data were processed with Origin Pro 2021b, the peaks, and the proper baseline with a slit width of 5 nm. Corresponding to L001-M sample showed peaks in 295 nm (2.1366), 320 nm (1.9977), 410 nm (0.7915), 615 nm (0.1304), 675 nm (0.2917) at 1.00 mg/mL. The absorbance of 0.10 mg/mL was not registered due to the system's sensitivity. L002-E extract shows peaks in 285 nm (2.0127), 325 nm (1.764), 405 nm (1.0545), 615 nm (0.1264), 675 nm (0.4029) at 1.00 mg/mL (See Figure 3.4).

In the Figure 3.4, the C003-M sample shows peaks in 410 nm (1.7553), 535 nm (0.4338), 615 nm (0.3251), 670 nm (0.6191) [1.00mg/mL]. While the C004-E extract show peaks in 415 nm (1.9286), 535 nm (0.4612), 615 nm (0.3473), 670 nm (0.6804) at 1.00mg/mL.

UV-Vis spectra analysis corresponds to recognizing peaks in the 200 to 400 nm. This region indicates the presence of sulfur (S), nitrogen (N), and oxygen (O), the presence of these elements indicate heteroatoms and unsaturated groups [42].

It used ethanol and methanol as solvents for our extracts because their maximum wavelengths are transparent in the UV-VIS region [43]. The L001-M and L002-E extracts have three peaks in this spectrum range, while C003-M and C004-E have one peak at 410 and 415 nm, respectively. These peaks confirmed the presence of chromophores. In fact,

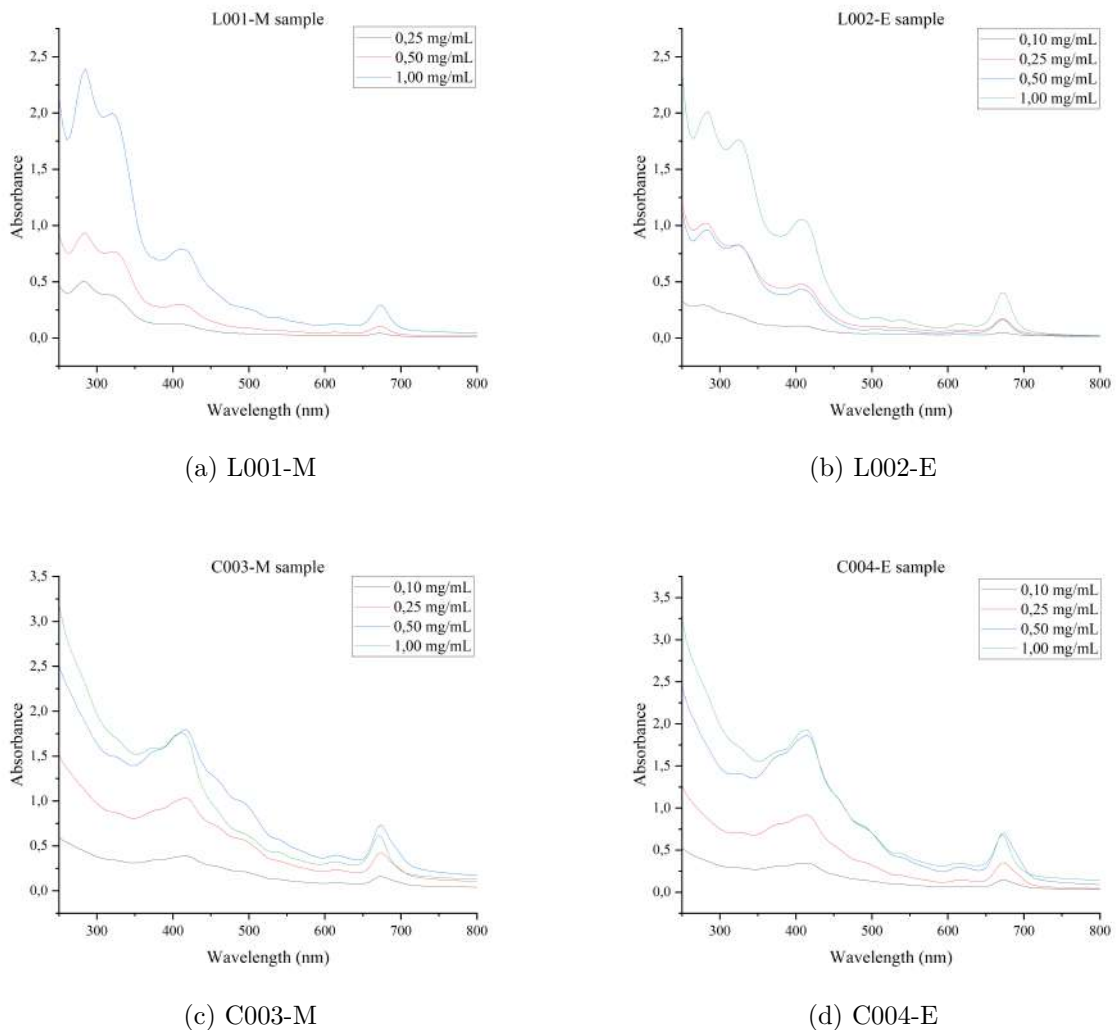


Figure 3.4: UV-VIS spectra of extract samples

the UV-VIS spectrum was used to identify components containing  $\sigma$  -bonds,  $\pi$  -bonds, lone electron pairs, and aromatic compounds [44]. According to the results of the two plants, it can be deduced that similar UV/Vis profiles are obtained, although the extraction solvent is different since the compounds are similar. Therefore the same entity is obtained in the signal. Therefore, corresponding to the data presented in Table 3.3., the wavelength number allowed identified the presence of different secondary metabolites [43, 44].

UV-Vis spectrum possibly identified metabolites corresponding to flavonoids at 320 nm and phenolic compounds at 280 and 360nm for extracts L001-M and L002-E. Notwithstanding C003-M and C004-E, the content of tannins, carotenoids, and terpenoids is highlighted. The peak absorbance of chlorophyll at 670 nm corresponds to the green/brown color that

Wavelength (nm)	L001-M	L002-E	C003-M	C004-E	Metablites
234-676	295	285	410	415	Alkaloids, flavonoids and phenol
	320	325	535	535	
	410	405	615	615	
	615	615	670	670	
	675	675			
230-350	295	285			Flavonoids and their derivates
	320	325			
350-500	410	405	410	415	Tannins, carotenoids and carotenoids
400-550			535	535	Terpenoids
600-700	675	615	615	615	Chorophyll
		675	670	670	

Table 3.3: UV-VIS profiles of secondary metabolites.

characterizes the extracts.

### NanoDrop analysis of extracts

The extracts were analyzed with the Nanodrop 2000 Spectrophotometer with the parameters of 1mm absorbance in a UV-visible wavelength range of 190 - 340 nm. It should also be noted that both extracts used were at a 1 mg/mL concentration using water type 1 to dilute for C003-M and C004-E and DMSO (1%) for L001-M and L002-E.

Figure 3.5 shows the spectrum for L001-M and L002-E, determined to have an absorbance peak at 200 nm near a 1.2 absorbance value. Both extracts have a similar absorbance profile; therefore, it showed they come from the same plant with different solvents of extraction in the maceration process. Evidence illustrates that certain secondary metabolites were found in higher proportions in the methanolic extract L001, confirmed in Figure 3.4.

Indeed, the C003-M sample (See Figure 3.6) has an absorbance of 0.5 at 200 nm, while C004-E shows an absorbance of 0.6 at the same wavelength. There was a higher absorbance in the 200-220 nm range in sample C003-M concerning C004-E. It was also identified that a peak was recorded at 240 nm, which may be related to the absorbance peak in Figure 3.4.

Nevertheless, each plant extract shows a similar profile across the spectrum, corresponding to extracts L001-M and L002-E corresponding to one plant and extracts C003-M

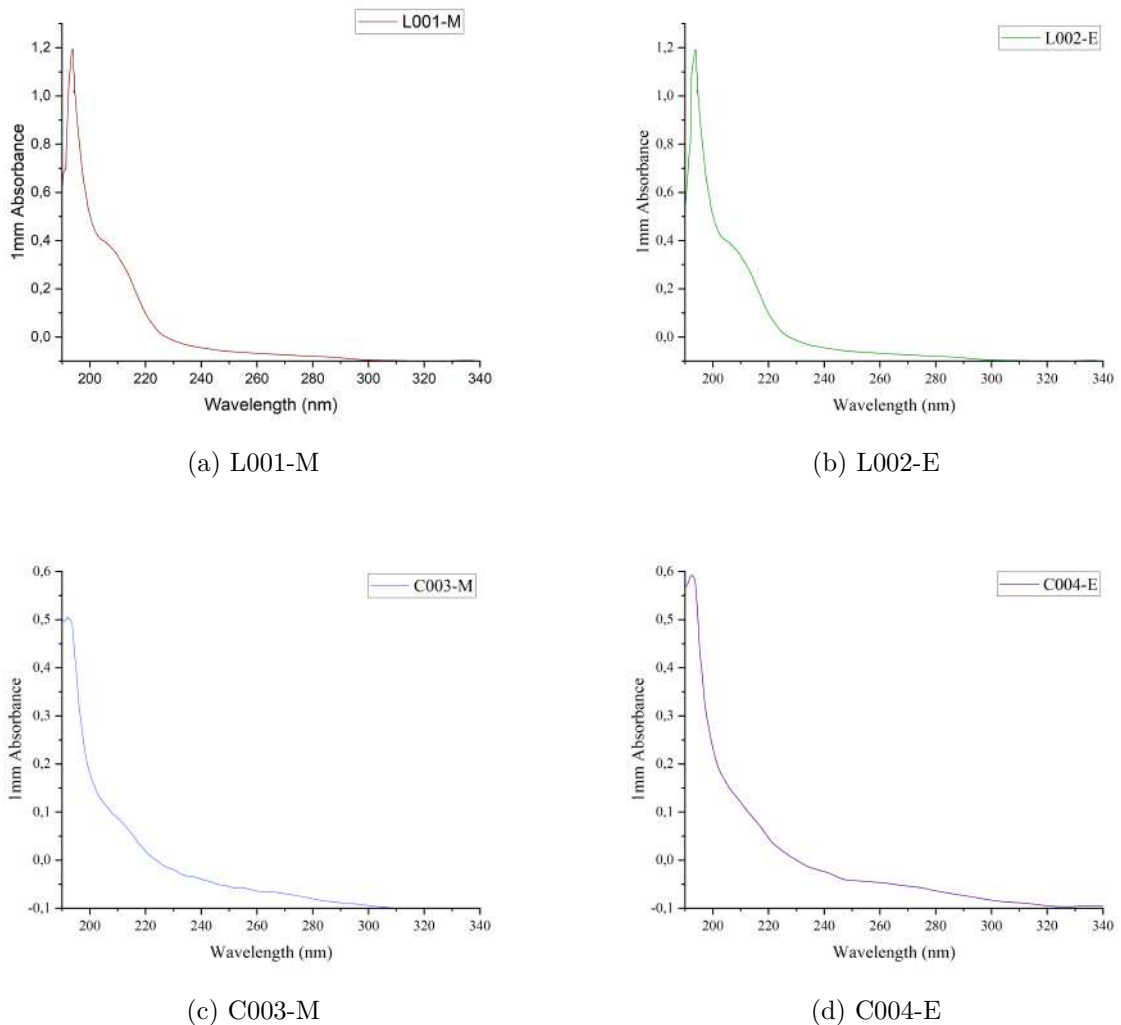


Figure 3.5: NanoDrop spectra of extract samples

and C004-M corresponding to another. The NanoDrop profile helped verify the samples' content after each extraction and characterization process.

### 3.5.2 FT-IR spectrum

The spectrum of FT-IR of all extracts was obtained in the infrared region with a wavelength of  $4000\text{cm}^{-1}$  and  $400\text{cm}^{-1}$ . This method is used for functional group identification by % transmittance value in the spectrum. A small quantity of L001-M, L002-E, C003-M, and C004-E were placed in the Cary 630 Fourier Transform Infrared Spectroscopy Spectrometer to elucidate the structure of the unknown composition, and the intensity of absorption spectra associated with molecular composition or chemical functional groups [45]. The

spectrum was registered from 4000 to 400  $\text{cm}^{-1}$  for each plant extract.

## Results and discussion

The FT-IR spectrum of the extracts is helpful to identify functional groups of the bioactive compounds by analyzing the % transmittance infrared radiation in the region registered. FT-IR spectra of L001-M (Figure 3.7) show a peak of  $3389.62 \text{ cm}^{-1}$  (63.241) assigned to the O-H stretching vibration designated to hydroxyl compounds, alcohols, and phenols. The peak at  $2927.76 \text{ cm}^{-1}$  (36.028) corresponds to the asymmetric stretching of -CH ( $\text{CH}_2$ ) vibration identified as lipids or saturated aliphatic compounds. The peak of  $2858.42 \text{ cm}^{-1}$  (63.332) corresponds to symmetric stretching of -CH ( $\text{CH}_2$ ) like fatty acids. The  $1696.98 \text{ cm}^{-1}$  (54,499) value corresponds to the C=O stretch assigned to a carbonyl group. The peak of  $1602.28 \text{ cm}^{-1}$  (68.896) belongs to the C=O stretching of the ketone compound. Indeed, the peak  $1518.93 \text{ cm}^{-1}$  (84.303) and  $1453.85 \text{ cm}^{-1}$  (67.143) is to C=C-C, and the aromatic ring corresponds to the aromatic compound. The  $1379.97 \text{ cm}^{-1}$  (69.760) corresponds to the O-H bend and alcoholic group for phenol or tertiary alcohol. The peak of  $1261.65 \text{ cm}^{-1}$  (63.625) corresponds to the C-O stretch, and the C-N stretch corresponds to acid or amino. The peak of  $1170.09 \text{ cm}^{-1}$  (65.950) corresponds to the C-H wag (- $\text{CH}_2\text{X}$ ). The peaks  $1067.89 \text{ cm}^{-1}$  (64.83) correspond to the  $\text{PO}_3$  stretch characterized by phosphate ions. Also, the peaks  $889.92$  (93.304),  $818.68$  (96.049), and  $756.07 \text{ cm}^{-1}$  (90.636) represent the =C-H, banding from alkanes. The peak  $710.90 \text{ cm}^{-1}$  (92.449) and  $602,90 \text{ cm}^{-1}$  (93.610) corresponding to =C-H and C-Cl are designated halogen compounds [46]. Values between brackets are their respective transmittance.

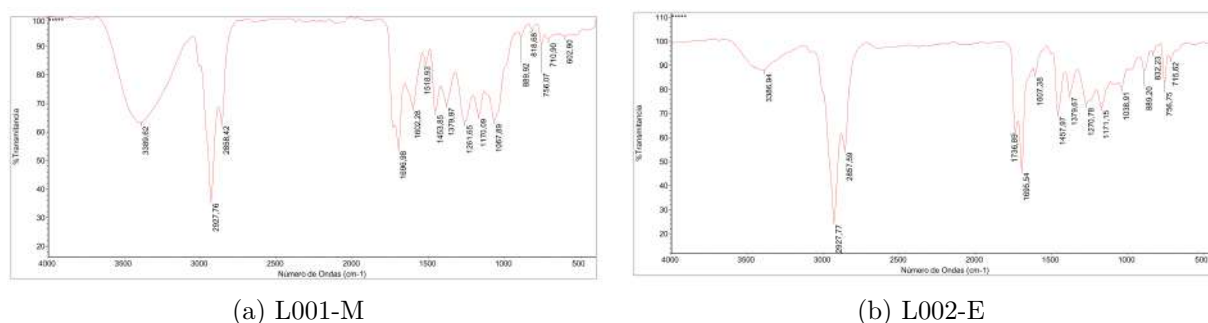


Figure 3.6: FT-IR of plant extracts

FT-IR spectra of L002-E (Figure 3.8) show a peak in  $3386.94 \text{ cm}^{-1}$  (88.048) assigned to the O-H stretch, carboxylic group, acidic, H-bonded, O-H stretch designated to carboxylic

acids, and hydroxy compounds, alcohols phenols. Indeed, the peak 2927.77 cm<sup>-1</sup> (24.999) assigned to the asymmetric stretching of -CH (CH<sub>2</sub>) vibration was designated to saturated aliphatic compound and lipids. The peak at 2857.59 cm<sup>-1</sup> (55.259) which are designated to the symmetric stretching of -CH (CH<sub>2</sub>) vibration corresponding to fatty acids, lipids, and protein. The 1736.89 cm<sup>-1</sup> (6.717) and 1695.54 cm<sup>-1</sup> (46,755) is related to C=O stretching of carbonyl group. The peak of 1607.38 cm<sup>-1</sup> (86.557) belongs to the C=O stretching of the ketone compound. The peak is 1457.97 cm<sup>-1</sup> (70.166) which is assigned to the C=C stretching corresponding to the aromatic compound. In addition, the peak of 1379.67 cm<sup>-1</sup> (78.149) is the O-H band, and the alcoholic group corresponds to phenol or tertiary alcohol. The 1270.78 cm<sup>-1</sup> (73.885) corresponds to the C-O stretch, C-N stretch corresponds to acid or amino. The peak 1171.15 cm<sup>-1</sup> (72.633) is assigned to the C-N stretch, C-H wag (-CH<sub>2</sub>X) of Amina, and alkylulides. The peaks 1038.91 cm<sup>-1</sup> (80.506) correspond to PO<sub>3</sub> stretching characterized by phosphate ions. Also, the peaks 889.20 (87.782), 832.23 (95.341), 756.75 (82.620) and 715.62 cm<sup>-1</sup> (92.947) represent the =C-H, banding from alkanes. 1261.65 cm<sup>-1</sup> (63,625) corresponds to the C-O stretch, and the C-N stretch corresponds to acid or amino. The peak of 1170.09 cm<sup>-1</sup> (65.950) corresponds to the C-H wag (-CH<sub>2</sub>X). The peaks 1067.89 cm<sup>-1</sup> (64.83) correspond to the PO<sub>3</sub> stretch characterized by phosphate ions. Also, the peaks 889.92 (93.304), 818.68 (96.049), and 756,07 cm<sup>-1</sup> (90.636) represent the =C-H, banding from alkanes. The peak 710.90 cm<sup>-1</sup> (92.449) and 602,90 cm<sup>-1</sup> (93.610) corresponding to =C-H and C-Cl are designated halogen compounds [47]. Values between brackets are their respective transmittance.

FT-IR spectra of C003-M (Figure 3.9) show a peak in 3352.40 cm<sup>-1</sup> (18.838) and 3010.64 cm<sup>-1</sup> (53.463) assigned to the O-H stretch, carboxylic group, acidic, H-bonded, O-H stretch designated to carboxylic acids, and hydroxy compounds, alcohols phenols. The peak at 2926.86 cm<sup>-1</sup> (9.922) and 2854.80 cm<sup>-1</sup> (35.885) is designated to the asymmetric stretching of -CH (CH<sub>2</sub>) vibration corresponding to saturated aliphatic compound and lipids. The 1741.07 cm<sup>-1</sup> (64.853) value corresponds to the C=O stretch assigned to the carboxyl group. The peak of 1600.45 cm<sup>-1</sup> (60.709) is the C=O stretching assigned to the ketone compound. The peak 1453.27 cm<sup>-1</sup> (61.191), assigned to the C=C-C, corresponds to the aromatic ring by the aromatic compound. The peak 1377.78 cm<sup>-1</sup> (61.780), assigned to the O-H band, is related to the alcoholic group corresponding to phenol or tertiary alcohol. The 1272.40

cm<sup>-1</sup> (69.146) corresponds to the C-O stretch, and the C-N stretch corresponds to acid or amino acids. The peak 1162.03 (61,354) cm<sup>-1</sup> is assigned to the C-H wag (-CH<sub>2</sub>X) and C-N stretching of amine and alkylidides. Also, the peak 1068.57 (42.149) cm<sup>-1</sup> is assigned to PO<sub>3</sub> stretching characterized by phosphate ions [48]. Values between brackets are their respective transmittance.

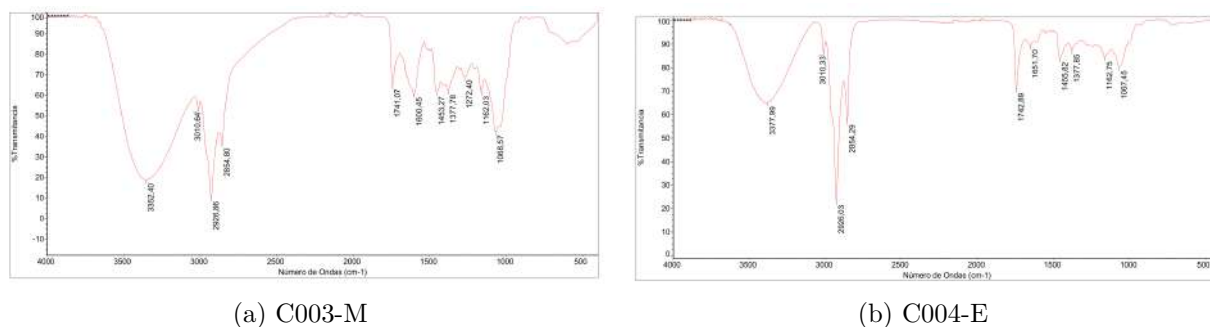


Figure 3.7: FT-IR spectra of extract samples

FT-IR spectra of C004-E (Figure 3.7) show a peak in 3377.99 cm<sup>-1</sup> (64.982) which is assigned to the H-bonded and O-H stretching vibration designated to hydroxy compounds, alcohols, and phenols. It shows a peak in 3010.33 cm<sup>-1</sup> (86.463), assigned to the C-H stretching designated to an aromatic group. The peak at 2926.03 cm<sup>-1</sup> (22.950) is designated to the asymmetric stretching of -CH (CH<sub>2</sub>) vibration corresponding to saturated aliphatic compound and lipids. The 2854,29 cm<sup>-1</sup> (57.084) value corresponds to the C-H stretch assigned to the alkanes and symmetric stretching of -CH (CH<sub>2</sub>) to fatty acids, lipids, and protein. The peak 1742.89 cm<sup>-1</sup> (70.706) is assigned to the C=O, corresponding to the carbonyl. The peak 1651.70 cm<sup>-1</sup> (88.792) is related to C=C stretching corresponding to the alkanes. Also, the peaks 1455.82 cm<sup>-1</sup> (83.559) are C=C stretching corresponding to the aromatic group. The peak 1377.85 cm<sup>-1</sup> (87.175) is assigned to the O-H band, and the alcoholic group corresponds to phenol or tertiary alcohol. The 1162.75 cm<sup>-1</sup> (84.177) is assigned to the C-N stretch, C-H wag (-CH<sub>2</sub>X) of Amina, and alkylidides. The peaks 1067.45 cm<sup>-1</sup> (80.270) correspond to PO<sub>3</sub> stretching characterized by phosphate ions. Values between brackets are their respective transmittance.

Thus to summarise, the results obtained are related to Table 3.2. corresponding to the phytochemical screening. The characterization of the secondary metabolites by FT-IR allowed evaluating of the possible functional groups of the chemical compounds of interest.

The O-H, -CH, O-H, C-O, C-N, PO<sub>3</sub>, C-Cl, C=C-C bonds may correspond to the stretching vibration designated hydroxyl compounds, alcohols, phenols, and aromatic phenols, amino groups, alkanes or phosphate ions by wavenumber [46]. Extracts L001-M and L002-E (see Figure 3.7.) are samples from the same plant with different solvents in the extraction step and showed similar peaks from 3600 cm<sup>-1</sup> to 2000 cm<sup>-1</sup>. The recorded result shows distinctive patterns in the fingerprint region (L001-M: C=C-C, phosphate, =C-H and C-Cl) compared to L002-E (C-O stretch, -CH<sub>2</sub>X). In comparison, the difference in transmittance (%) between samples C003-M and C004-E of the extract in the region (2500-3500 cm<sup>-1</sup>) could be affected by chlorophyll (type A and B) and carotenes, while in the fingerprint region, it was registered in C003-M (C-O stretch) corresponds to acids or amino acids.



# Chapter 4

## Biological activity: antibacterial, antioxidant and anti-inflammatory

### 4.1 Reagents and equipment

The reagents used for *in vitro* antibacterial, antioxidant and anti-inflammatory activity correspond to sodium chloride ( $\geq 99.5\%$ , Merck), potassium ferricyanide ( $\geq 99\%$ , Merck), sodium chloride (99.9%, Merck), hydrochloric acid (37%, Merck), trichloroacetic acid (99%, Merck), sodium phosphate ( $\geq 99\%$ , Sigma Aldrich), dimethyl sulfoxide ( $\geq 99\%$ , Sigma-Aldrich), chloroform ( $\geq 99.5\%$ , Sigma-Aldrich), potassium chloride (99%, Sigma-Aldrich), ferric chloride ( $\geq 98\%$ , Sigma-Aldrich), Kanamicyn sulfate (powder, Sigma-Aldrich), disodium hydrogen phosphate (99.5%, Scharlau), potassium dihydrogen phosphate ( $\geq 98\%$ , Fisher scientific), commercial tube EDTA-K3 VanTubo<sup>o</sup> sterile (Van Chiang IND. CORP.), Luria Bertani Broth, Miller (Titan Biotech LTD), and Luria Bertani Agar, Miller (Titan Biotech LTD).

*In vitro* antibacterial, antioxidant and anti-inflammatory activity equipment used was UV/Vis/NIR Spectrophotometer Lambda 1050 (PerkinElmer, USA), NanoDrop<sup>TM</sup> 2000 Spectrophotometer (Thermo Scientific<sup>TM</sup>, USA) and MaxQ<sup>TM</sup> 4450 Benchtop Orbital Shaker (Thermo Scientific<sup>TM</sup>, USA).

## 4.2 Antibacterial activity: Minimum Bactericidal Concentrations (MBC's)

### Bacterial strain and inoculums preparation

The antibacterial potency of each plant extract was evaluated using the bacterial strain of Gram-negative bacteria (*E. coli*) called TG1, DH5- $\alpha$ , and E410A5. The media Luria Bertani Broth, Miller showed is suitable for growing the bacteria. Using Luria Bertani Broth, Miller, the bacteria TG1, DH5- $\alpha$ , and E410A5. were subcultivation overnight at 37 °C with 160 revolutions per minute [49].

### Antibacterial screening

The L001-M, L002-E, C003-M, and C004-E plant extracts were dissolved in 3 mL of distilled water to evaluate the antimicrobial activity. and the concentration from the extract used was 0.1 mg/mL, 0.25 mg/mL, 0.5 mg/mL, 1.0 mg/mL, 1.5 mg/mL, 2.5 mg/mL, 5 mg/mL, 10mg/mL, 15mg/mL and 20mg/mL. Based on the standard McFarland turbidity values, a value of 3 was obtained, approximate cell density ( $1 \times 10^8$  CFU/mL) by a factor of 9. This value was obtained after measuring OD600 equal to 0.602 absorbance measurement on NanoDrop™ 2000 Spectrophotometer. [50]. Luria Bertani agar medium (250 mL) was pured in several sterile Petri dishes (approximately 35 mL), and 300 ul of bacteria strain was seeded in a medium previously prepared with bacterial suspension. Then, different extracts concentrations were placed on the top of Luria Bertani Agar, Miller plates. Kanamycin was used as the positive control for well-known antibacterial capacity at 50 mg/mL. The samples were incubated at 37 °C for 24 hours. If there is an inhibition halo, it is considered an indication of antibacterial activity.

### Results and discussion

The antibacterial activity of the extracts was assayed by the qualitative method with TG1, DH5- $\alpha$ , and E410A5 cell lines. The extracts showed the inhibition halo (ZI) against all gram-negative bacteria. The extract L001-M and L002-E were effective against DH5- $\alpha$  (See Figure 4.2.). The same extracts showed no activity against TG1 and E410A5 (gram-negative bacteria). None of the extracts C003-M and C004-E showed antimicrobial activity. The L001-M showed excellent antibacterial activity against DH5- $\alpha$  at a 2.5 mg/mL concentration, as the L002-E (See Figure 4.1.).

Plant extract	Inhibition halo (mm)						Positive Control	Negative Control
	1.5 mg/mL	2.5 mg/mL	5 mg/mL	10 mg/mL	15 mg/mL	20 mg/mL	K* 50 mg/mL	W-1**
L001-M	-	1.9	2.6	2.8	2.3	2.5	13.0	-
L002-E	-	0.9	2.1	2.3	2.0	1.8	15.0	-

\*Kanamycin \*\*Water type 1 sterile

Table 4.1: Antimicrobial screening test of effective extract against DH5- $\alpha$ .

The inhibition zone was measured, and the results are shown in Table 4.1. The different inhibition zone values depend on the concentration of the extract and the chemical and volatile nature of the bioactive constituents (See Figure 4.1.). It is detailed that the Minimum Bactericidal Concentration is 2.5 mg/mL for L001-M and L002-E extracts. This suggested that the functional groups identified by FT-IR in the methanolic and ethanolic extract of L001-M and L002-E efficiently suppress the DH5- $\alpha$  cell line.

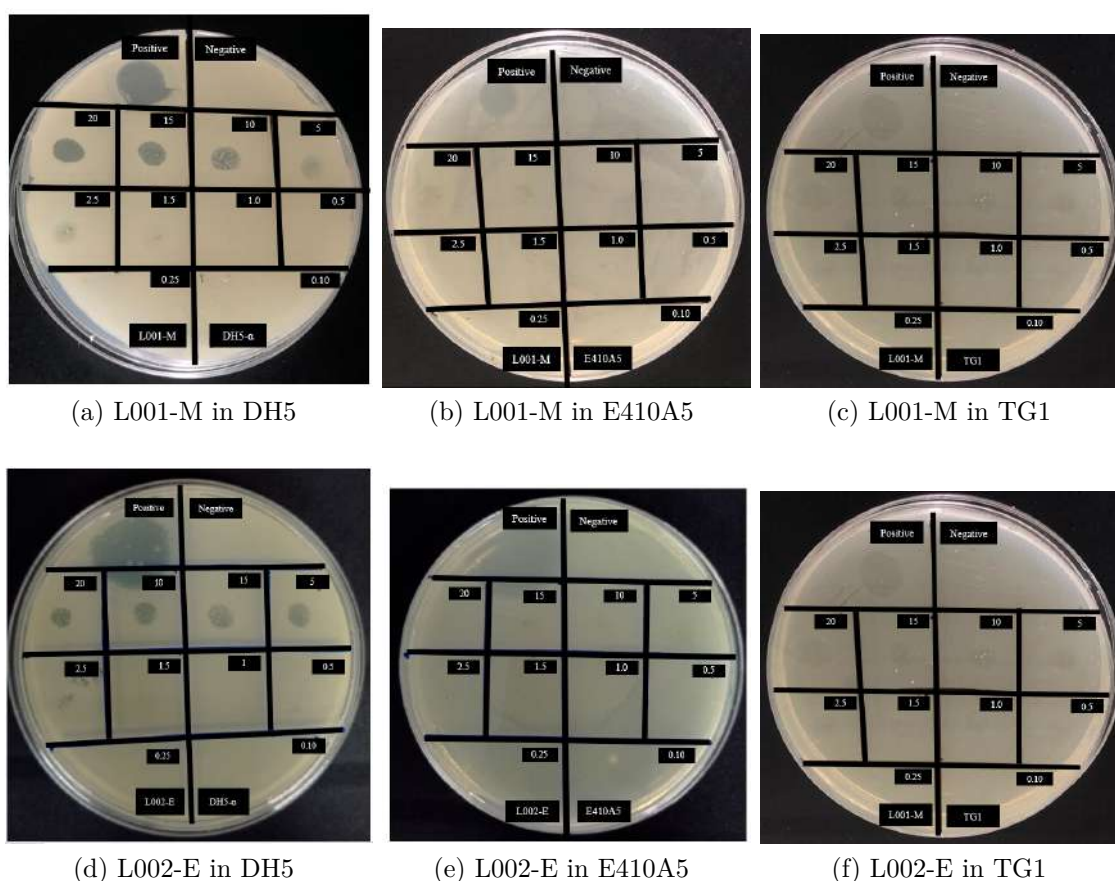


Figure 4.1: Antibacterial activity of the plant extract.

Microsoft Excel 2016 statistical package was used to analyze the data using the  $t$ -

test statistic with a significance level of 0.05. The significant antimicrobial effects were expressed in Table 4.1. they correspond to the L001-M extract compared to the effect of the positive control. Similarly, L002-E shows a significant difference concerning the antibacterial effect of kanamycin. As put forward by [15], the difference in the inhibition halo value corresponded to the variation of chemical constituents and the volatile nature of plant extract components.

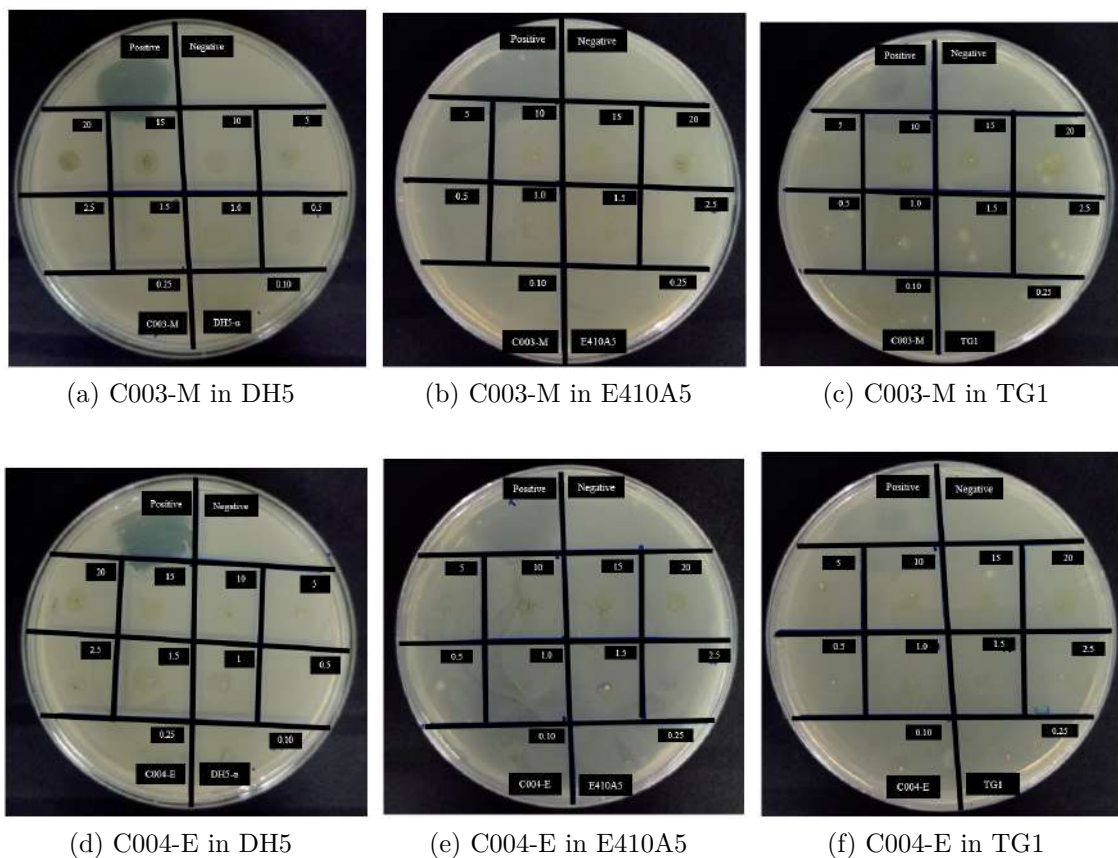


Figure 4.2: Antibacterial activity of the plant extract.

It was observed that C003-M and C004-E extract had no antibacterial activity for TG1, DH5- $\alpha$ , and E410A5 cell lines (See Figure 4.2.). This method of antibacterial activity is affected by the complex bioactive components of extracts. Therefore, factors such as inoculum size and concentration may produce a large area of inhibition at lower concentrations, while a thick layer of cells may produce a much smaller inhibition halo or false negatives [51]. These bacteria were chosen due to *E. coli* had been isolated from infected wounds and wound infections. Moreover, gram-negative showed quite high resistance to the majority

of antibiotics [52]. As a result, extracts L001-M and L002-E can be used in biomedical applications related to wound infections.

### 4.3 Relative Antibacterial Capacity

#### Bacterial strain and samples preparation

The relative antibacterial activity of L001-M and L002-E plant extracts was evaluated using one Gram-negative strain (*Escherichia coli*) called DH5- $\alpha$  because qualitatively antibacterial essays show inhibition of this bacteria growth. For cell culture optical density measurements, NanoDrop™ 2000 Spectrophotometers were used based on *in vitro* time-kill methodology bioassay experiments [53]. The blank was an LB-broth culture medium, and the wavelength measurement was 600 nm. The positive control was Kanamicyn at 20 mg/mL concentration for this antibacterial essay. In the same way, the negative control was LB broth culture plus bacteria without antibiotics and extract. Therefore, the plant extract was prepared at 20 mg/mL of concentration for L001-M and L002-E samples.

#### Inoculation and procedure

Using Luria Bertani broth agar slants, the 25 uL of DH5- $\alpha$  bacteria were cultivated at 37°C with 160 revolutions per minute for 24 hours [49]. The volume taken from the initial bacterial suspension was calculated with the following formula of concentration-optical density correlation. In the beginning, the OD600 value of DH5- $\alpha$  was 0.456, but it needed 0.02 as the initial concentration for this experiment. Therefore, to calculate the inoculation volume for dilution, equation (3) is:

$$C_1 * V_1 = C_2 * V_2 \quad (3)$$

where  $C_1$  and  $V_1$  refer to stock cell concentration which is the initial bacterial suspension, and  $C_2$  and  $V_2$  are the final concentration for the experiment, which in this case, the absorbance obtained from DH5- $\alpha$  is the initial absorbance and it is proportional to the concentration modifying the formula equation (4) is obtained:

$$A_{1DH5} * V_{1DH5} = A_{2DH5} * V_{2DH5} \quad (4)$$

Where  $A_{1DH5}$  is the stock bacteria absorbance (0.456),  $V_{1DH5}$  is the stock bacteria volume which is necessary to add for final concentration,  $A_{2DH5}$  is OD600 required absorbance value (0.02), and  $V_{2DH5}$  is the final volume in the cell culture tubes (2 mL)—replacing the values in the equation, the tubes were filled with 89 L of DH5- $\alpha$  initial bacterial suspension.

## Results and discussion

After inoculation, cell culture tubes were taken to the MaxQ™ 4450 Benchtop Orbital Shaker at 180 rpm and 37 °C. Once there, an aliquot of 9 uL was used from each cell culture tube every half hour to measure the OD600 value. The results were processed and plotted in Figure 4.3. The total time of experimental measurements was 5 hours.

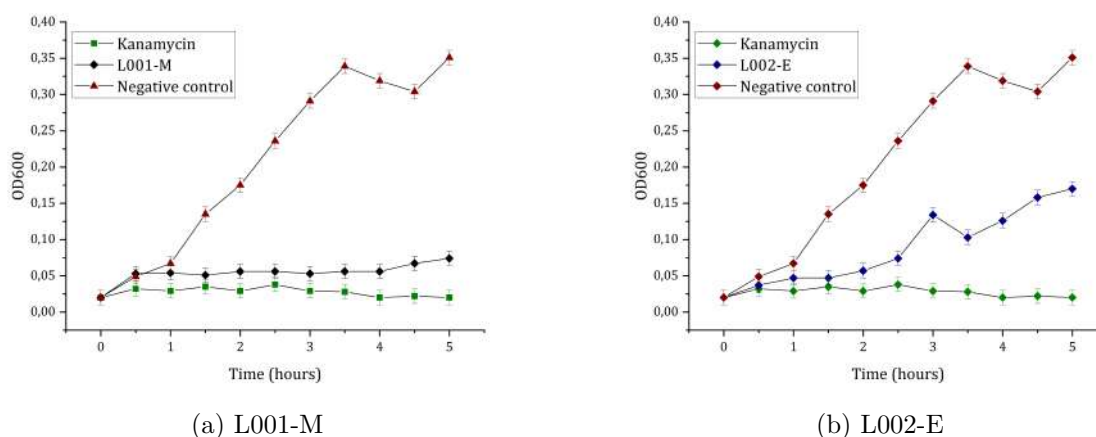


Figure 4.3: Bacterial growth curves formed from OD600 measurements of extracts

As a matter of fact, the cell density is directly proportional to the optical density. Therefore, as predicted, the negative control OD600 value where LB broth culture with bacteria usually grows. In particular, L001-M showed an antibacterial activity similar to that of kanamycin positive control at 20 mg/mL of concentration. However, sample L002-E showed low antibacterial activity with values intermediate between the positive and negative control. The results were analyzed using *t*-test statistical tool, indicating a significant difference between the L001-M and antibiotic activity. In other terms, there was no relationship between plant extract L001-M and kanamycin antibacterial activity. Indeed, it was statistically analyzed that the L002-E extract is significantly different for both the positive and negative control. Regarding, results suggested the antibacterial activity of L002-E decreases with respect to time, demonstrating that methanolic solvent

extraction had a better antibacterial effect than ethanol extraction (See Figure 4.3).

These antibacterial results demonstrated the previously reported L001-M and L002-E extracts' antibacterial activity and verified that the studied plant is a potential resource with potential antibiotics applications in the pharmacological field.

## 4.4 *In vitro* antioxidant activity

### Preparation of extracts and standard

Extracts samples L001-M, L002-E, C003-M, and C004-E were evaluated by ferric reducing power and Total antioxidant activity by phosphomolybdenum methods. The four plant extracts were prepared on the concentrations of 0,05 mg/mL, 0,1 mg/mL, 0,25 mg/mL, 0,5 mg/mL, 1 mg/mL, 1.5 mg/mL and 2.5 mg/mL in distilled water. The standard reagent was ascorbic acid at 0.001 mg/mL, 0.05 mg/mL, 0.1 mg/mL, 0.25 mg/mL and 0.50 mg/mL for the assays. Three replicates of each sample were prepared for assay. A blank was prepared without adding the extract to the antioxidant complex.

#### 4.4.1 Ferric Reducing Power assay (FRP)

Ferric reducing antioxidant power was performed to determine  $Fe^{3+}$  to  $Fe^{2+}$  by measuring the absorbance of sample and standard in 700 nm by UV-VIS spectrophotometer because it is the absorption maximum to the ferric, ferrous complex [54] (See Figure 4.4.). The antioxidant compound in the extracts was recognized by the antioxidant assay activity recorded for forming complexes with the metal atoms present, specifically copper and iron [55]. The increase in absorbance value is proportional to the antioxidant activity.

The calibration curve equation for FRP analysis based in the resulting absorbance versus concentration was obtained using equation (5):

$$y = mx + b \quad (5)$$

where  $\mathbf{m}$  is the slope and  $\mathbf{b}$  is the y-intercept.

The reduction phenomena was expressed in  $\mu\text{g}$  ascorbic acid equivalents/g by the equation (6) [56]:

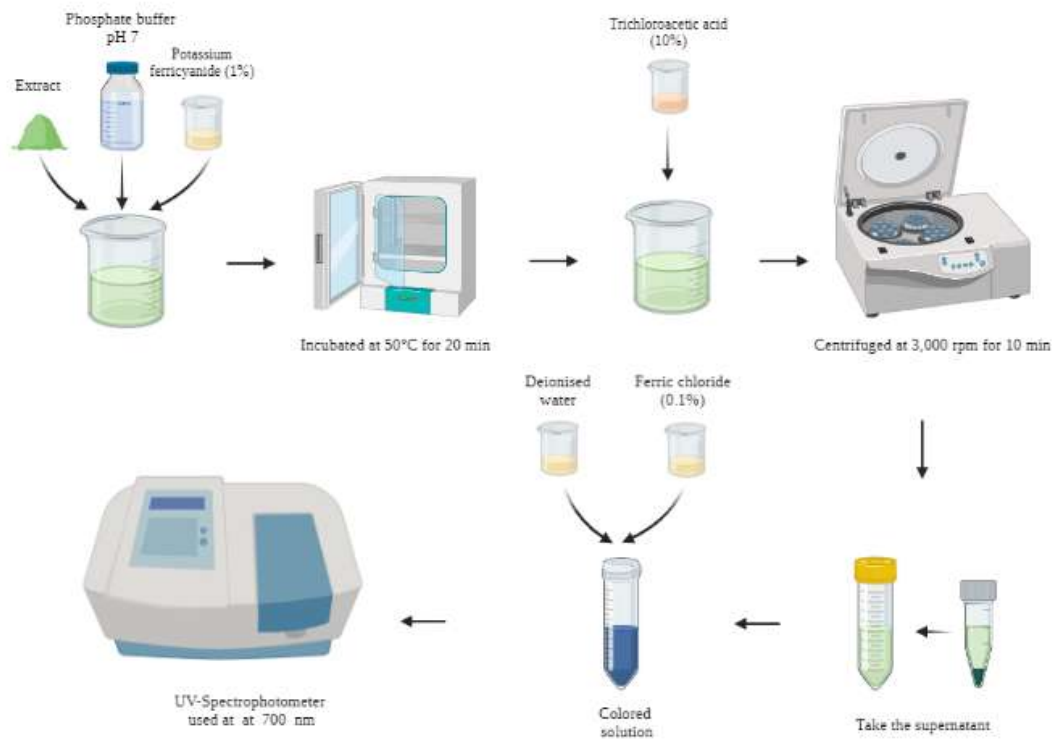


Figure 4.4: Ferric reducing power assay procedure

$$AEAC_{\frac{mgAA}{g}} = \frac{(registeractivityextract)(factordilution)(V_{sample}(mL))}{g_{sample}} \quad (6)$$

with AEAC = ascorbic acid equivalent antioxidant activity,  $\mu gAA$  microgram of ascorbic acid and. Further, activity is obtained from calibration curve with the equation (7):

$$Activity_{\frac{xmg}{mL}} = \frac{y - b}{m} \quad (7)$$

Therefore, the percentage of reducing power (%RP) calculated from the following equation (8) [56]:

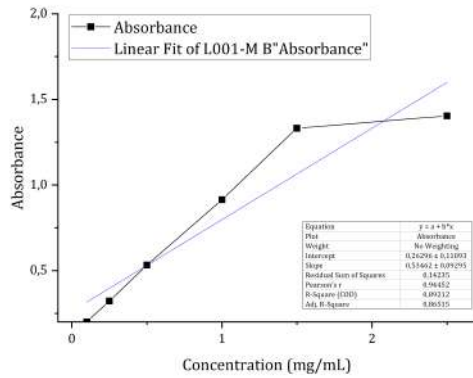
$$\%RP = [1 - (1 - \frac{A_e}{A_a})] * 100 \quad (8)$$

where RP is reducing power,  $A_e$  is absorbance of extract and  $A_a$  is absorbance of ascorbic acid.

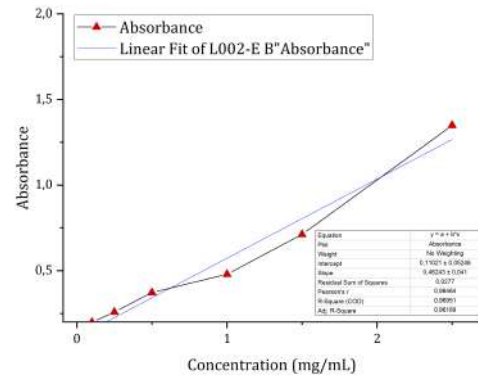
## Results and discussion

To measure the reductive ability, the  $Fe^{3+}$  to  $Fe^{2+}$  transformations in the presence of

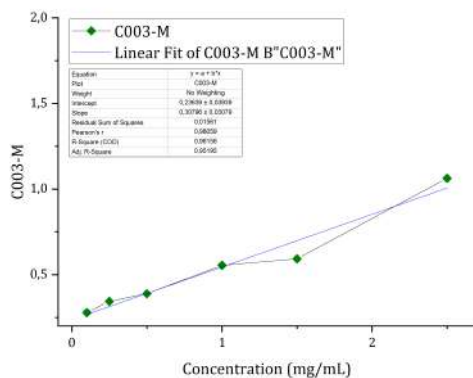
the four plant extract with the complex of potassium ferricyanide, trichloroacetic acid, and ferric chloride was investigated. The yellow color changed to green or blue depending on antioxidant power presented in the experiment result from [57].



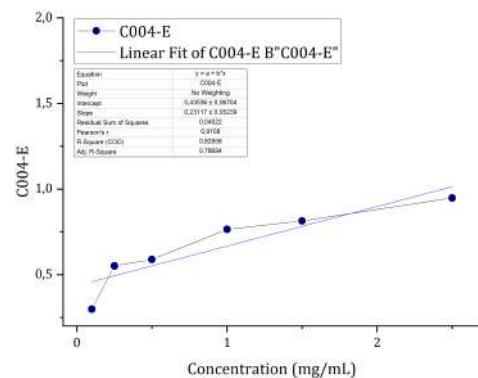
(a) L001-M



(b) L002-E



(c) C003-M



(d) C004-E

Figure 4.5: The absorbance of plant extract in Ferric Reducing Power determination.

The method showed to be useful for antioxidant capacity through a screening and comparison of the extraction solvents. Ferric reducing antioxidant reaction shows good linear relation in both ascorbic acid as standard and sample extract (See Figure 4.5.). Indeed, L001-M showed more absorbance value as a signal of antioxidant activity compared to L002-E in the FRP assay. The reducing power increase according to the increasing concentration of the extracts. The  $R^2$  value for L001-M is 0.89 and for L002-E is 0.97, indicating that the second extract adjusted better to the linear behavior as the standard.

On the other hand, the ferric reducing power of C003-M and C004-E show an an-

tioxidant ability for the transformation of  $Fe^{3+}$  into  $Fe^{2+}$  when yellow transforms into blue/green [58]. The measurement of Perl's Prussian (blue color) at 700 nm reflects good linearity of C003-M (0.96) compared to C004-E (0.82). To analyze FRP results was necessary to perform a calibration curve from ascorbic acid (See Figure 4.6.).

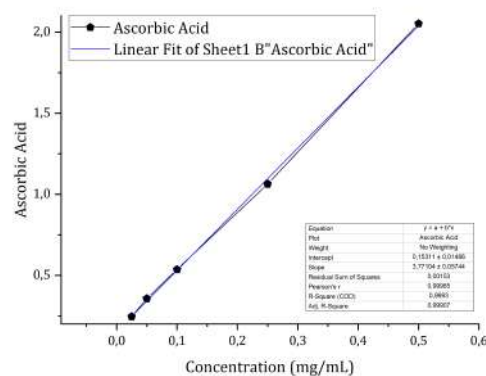


Figure 4.6: Ferric Reducing Power assay procedure

Replacing the ascorbic acid values in the equation (5):

$$y = 3.77104x + 0.15311$$

with excellent  $R^2$  value of 0.99.

Then the reduction phenomena was obtained reemplazando los valores de m y b en la equation (7):

$$Activity_{\frac{x_{mg}}{mL}} = \frac{absorbance - 0.15311}{3.77104}$$

In this essay, the absorbance value of the sample at 2.5 mg/mL was used to analyze antioxidant activity. The percentage of reducing power (%RP) was calculated using the equation (8). The results are presented in Table 4.2:

Plant extract	FRAP value in AEAC (mg AA/g)	Reducing power (%RP)
L001-M	7.96161	68.40925
L002-E	7.600568	65.68412
C003-M	5.790381	51.78725
C004-E	5.060821	46.20219

Table 4.2: FRAP value in AEAC (mg AA/g) and Reducing power (%RP)

Evidence illustrates that the extract L001-M had a remarkable potency to donate electrons to the reactive free radicals; this causes the non-reactive species to become more stable, culminating in the chain reaction characterized by free radicals [59]. The %RP of L001-M and L002-E is higher than the C003-M, and C004-E extracts, and the methanolic extractions, show higher antioxidant activity. There was no statistically significant difference between the reducing power of L002-E and L001-M. Consequently, differences are statistically significant if the reducing power percentage of L001-M is compared with the C003-M and C004-E. Correspondingly, the reducing power in the FRP assay is dependent on the plant's chemical components due to the previous characterization.

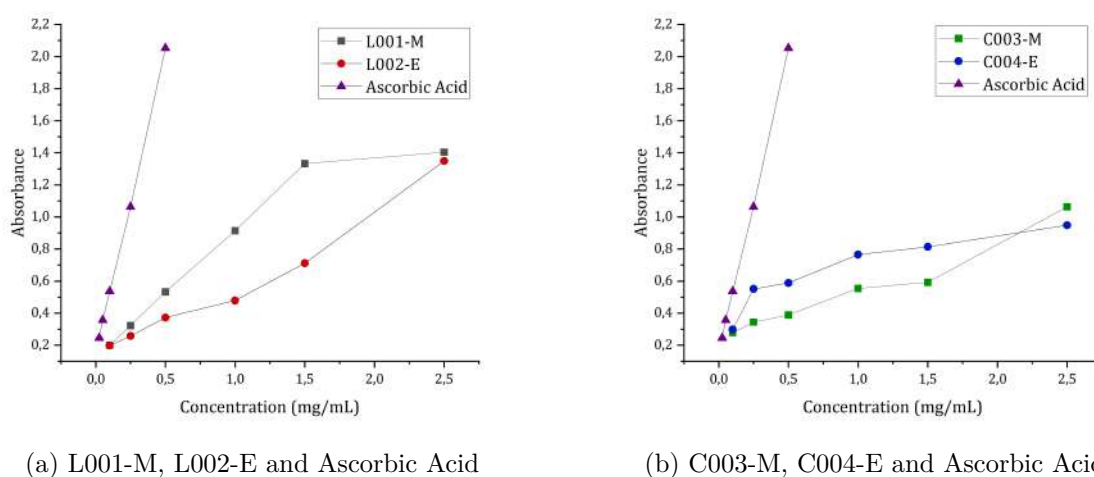


Figure 4.7: Ferric Reducing Power results comparison of plant extract and standard

The FRP is under the standard reagent in the case of L001-M and L002-E extract. However, excellent antioxidant activity was recorded compared to the extracts C003-M and C004-E (See Figure 4.7.). Thus, the antioxidant ability of the extracts in inhibiting the oxidative effects of reactive oxygen species found in the reaction mixture was tested through the colorimetric method.

#### 4.4.2 Total Antioxidant Activity (TAC) by phosphomolybdenum method

The chemical principle to assess the total antioxidant capacity based on the plant extract possessing antioxidant compounds through reduction of Mo (VI) to Mo (V) [60]. The

chemical complex allowed to measure of the Total antioxidant activity by phosphomolybdenum method (TAC). The extracts were evaluated according to the method described in [61] for antioxidant capacity (Figure 4.8). Samples and standards were prepared at the same concentration that the previous FRP assay.

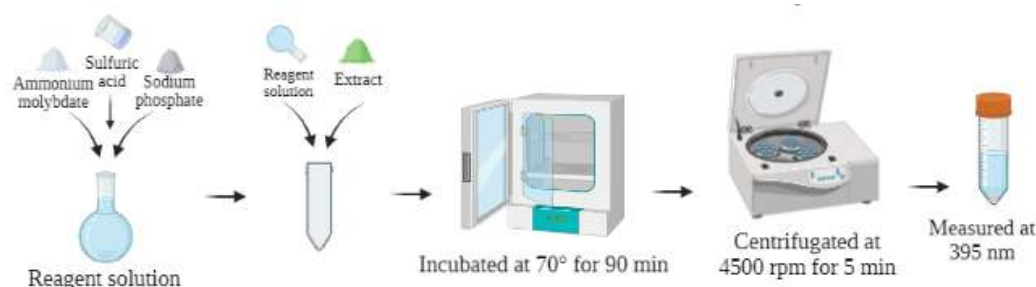


Figure 4.8: Total antioxidant activity by phosphomolybdenum method

## Results and discussion

After the extracts were added to the solution, Mo (VI) was reduced to Mo (V). This is shown by the green coloration change indicating phosphomolybdenum complex V whose absorbance was measured at 695 nm using UV/VIS/NIR Lambda 1050 spectrophotometer [62]. The total antioxidant activity is expressed in the gram equivalent of ascorbic acid [63] as well as the calibration curve was with ascorbic acid.

The samples L001-M and L002-E show suggest that the extracts had the potential as free radical scavengers (See Figure 4.9.). First, L001-M showed excellent total antioxidant activity compared to L002-E. The  $R^2$  of L001-M is 0.98 and for L002-E is 0.99, which shows that extracts used in the assay have a good linear fit, as was expected.

The TAC essay of C003-M and C004-E plant extract had similar antioxidant activity. The value of  $R^2$  for C003-M is 0.98, while C004-E was 0.95.

Total antioxidant activity is compared with the values of the ascorbic acid calibration curve to express in gram equivalent of ascorbic acid (See Figure 4.6.). Using the same procedure as in ferric reducing power assay, with the slope-order  $y = 3.77104x + 0.15311$  as well as an  $R^2$  equal to 0.99. The total antioxidant activity was calculated for the extracts' highest concentration and the standard's highest concentration. The following results are obtained in Table 4.3.

The results could suggest the plant extracts' antioxidant capacity, highlighting that the sample L001-M has the highest TAC compared to others. The compounds of the

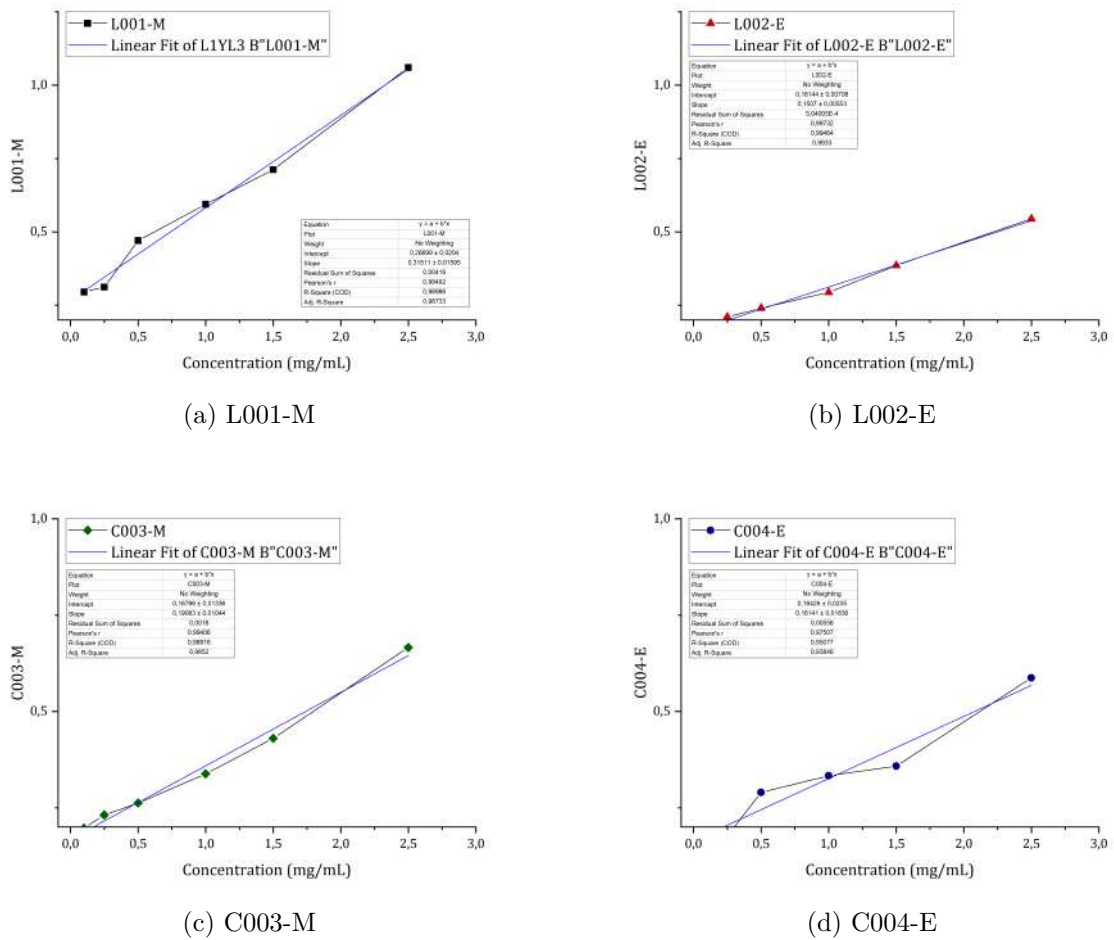


Figure 4.9: Total antioxidant activity of plant extracts

extracts that may be involved in the TAC are flavonoids, carotenoids, and cinnamic acid derivatives [61, 60]. This type of assay allows for determining the antioxidant activity of the extract, although more specific techniques are suggested to understand the activity of each secondary metabolite and its identification.

The *t*-Test was used to analyze the difference between the four extracts with a confidence level of 95%. Overall, the L001-M extract (99.76%) showed the highest total antioxidant ability compared to the other extracts. L002-E, C003-M, and C004-e were non-significantly correlated compared to L001-M. Otherwise, the methanolic extractions were found to contain more antioxidant agents compared to ethanolic extractions. However, L001-M and L002-E were the same plants and detected the same classes of phytochemicals. The quantitative difference could result from the heterogeneous concentration of the

Plant extract	Total antioxidant activity (%)
L001-M	99.76168
L002-E	51.23863
C003-M	62.67481
C004-E	55.24929

Table 4.3: Total antioxidant activity of plant extracts

phytochemicals. The overall antioxidant findings warrant further studies on the different isolation techniques and characterization of the secondary metabolites responsible for antioxidant activity.

## 4.5 *In vitro* anti-inflammatory activity

### Preparation of extracts

The required concentrations of 0.05 mg/mL, 0.1 mg/mL and 0.25 mg/mL of plant extracts were prepared. The same concentration for the positive control was aspirin. In addition, the negative control of samples L001-M and L002-E samples were diluted with DMSO (1%), while for extracts C003-M and C004-E, it was water type 1.

### Preparation of blood samples for membrane stabilization tests

Human red blood cell (HRBC) has been used for anti-inflammatory *in vitro* studies [64]. Blood was obtained from a volunteer with the restriction to not consume any anti-inflammatory drug fourteen days before the test. Therefore, a 5 mL commercial tube with EDTA-K3 VanTubo and a sterile needle were employed; 15 mL (3 dips) of human blood was obtained and slowly mixed between the coagulant and the blood. The Solca Hospital Ethics Committee has already approved the experiment.

Therefore, it was centrifuged at 3000 rpm for 5 minutes, and the supernatant was eliminated. Next, the cell suspension was washed with saline solution (0.9% w/v NaCl) and centrifuged at 3000 rpm for 5 minutes; threefold. Finally, the last resuspension with 40% (v/v) of phosphate-buffered saline solution (1x PBS Buffer) at pH 7.4.

### Hemolysis induced by hypotonicity

For this procedure, 2 mL of saline solution at 0.9%, 1 mL of phosphate-buffered saline, and 1 mL of L001-M, L002-E, and C004-E extract, respectively. Subsequently, 500  $\mu$ L of the blood process was added to the falcon tube. For the L001-M and L002-E samples,

the negative control contains a DMSO (1%) in distilled water. The negative control for C003-M and C004-E was water type 1. Also, aspirin was used as a positive control at the same concentrations of plant extracts (0.05 mg/mL, 0.1 mg/mL and 0.25 mg/mL). Then, samples were incubated for 30 minutes at 37 °C, and tubes were centrifuged for 20 minutes at 3000 revolutions per minute. The supernatant was collected, and the absorbance of each solution was measured on a 560 nm as an indicator of the degree of hemolysis [65].

### Percentage of hemolysis inhibition

The equation (9) was used to calculate the percentage of inhibition of hemolysis [66]:

$$\text{Inhibition of hemolysis} = \left[ \frac{(OD_W - OD_E)}{(OD_W)} \right] * 100 \quad (9)$$

Where  $OD_W$  is the optical density of the hypotonic buffer without extract, and  $OD_E$  is the optical density of the hypotonic buffer with the extract.

### Results and discussion

The analysis for L001-M and L002-E was applied using the formula of percentage inhibition of hemolysis; the following results have been analyzed. In the Figure 4.10. aspirin, L001-M, and L002-E extract demonstrated anti-inflammatory activity. The range of inhibition of hemolysis induced by hypotonicity at different concentrations of LO01-M and L002-E is in the range of 8% to 30% of inhibition of hemolysis. Specifically, L001-M, which is the methanolic extract of the plant at 0.05 mg/mL, represented the highest value of inhibition of hemolysis, while at higher concentrations, possibly the synergism of various metabolites decreases, as working with complete extracts may result in all at high concentrations.

The results show increasing antioxidant and anti-hemolytic activity of L001-M plant extract. The plant extract's anti-inflammatory effect reduced the hemolysis magnitude when red blood cells were exposed to toxic reagents. The statistical analysis was applied using 0.05 mg/mL of aspirin as a positive control. The L001-M was not significantly different from aspirin's anti-inflammatory effect. In contrast, extract L002-E showed a significant difference compared with the control.

Indeed, the anti-inflammatory activity of C004-E extract had the effect of inhibiting the hypotonicity-induced hemolysis in healthy erythrocytes. The trend is the same as in

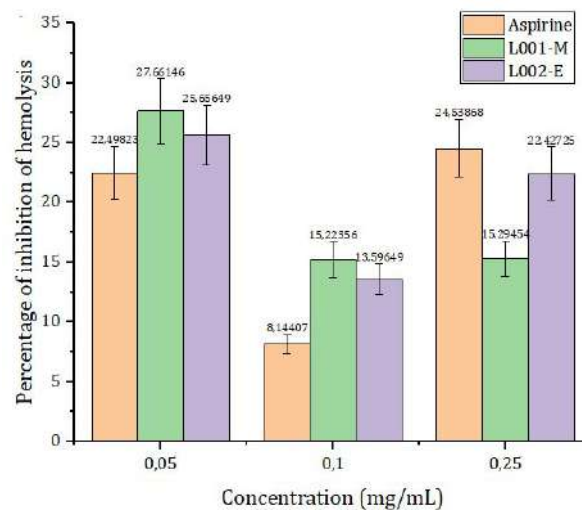


Figure 4.10: Anti-inflammatory activity of the plant extract comparing its effectiveness with the commercial Aspirin.

the previous case; the optimum concentration of the extract was 0.05 mg/mL.

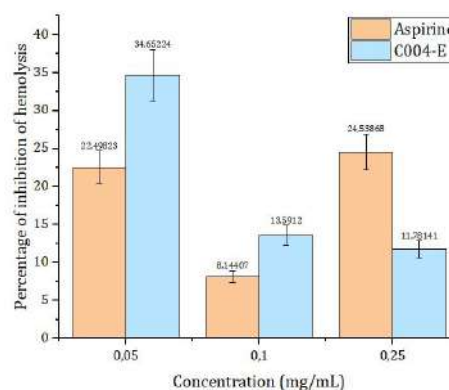


Figure 4.11: Anti-inflammatory activity of the plant extract comparing its effectiveness with the commercial Aspirin.

In Figure 4.11., C004-E extract showed higher anti-inflammatory activity than L001-M and L002-E. Indeed, small dips are made in each centrifuge, and it does not shake because the erythrocyte membrane breaks. Through *t*-Test, it was founded that Aspirin and C003-E extract did not show significant differences. Results may be related to the different chemical compounds of the extract and the functional groups previously identified in the characterization process.

However, the extracts were shown to decrease the stress induced on the plasma membrane to be destroyed. The presence in the extracts of biomolecules such as flavonoids

and phenols may be responsible for this biological activity [67]. However, the therapeutic mechanism of the extracts on erythrocytes is not precisely understood.



# Chapter 5

## Development of hydrogels using botanical extracts

### 5.1 Reagents and equipment

The reagents used for the hydrogels samples using botanical extracts corresponds to Sigma Cellulose Type 101 Cellulose (Sigma Aldrich, USA); microcrystalline cellulose (Alfa Aesar, USA), potassium chloride (99%, Sigma-Aldrich), disodium hydrogen phosphate anhydrous (99.5%, Scharlau), potassium phosphate monobasic ( $\geq 99.6\%$ , Fisher scientific).

The hydrogel synthesis and characterization equipment used were Cary 630 Fourier Transform Infrared Spectroscopy Spectrometer (Agilent, USA); UV/Vis/NIR Spectrophotometer Lambda 1050 (PerkinElmer, USA), MaxQ™ 4450 Benchtop Orbital Shaker (Thermo Scientific™, USA) and M205-C Stereo Microscope (LEICA, Switzerland)

### 5.2 Synthesis and characterization of hydrogel

#### 5.2.1 Cellulose hydrogel synthesis

This section aims to create cellulose hydrogels with the L001-M, L002-E, C003-M, and C004-E to study their use in biomedical applications. Sigma Cellulose Type 101/cotton cellulose (NRC) and Microcrystalline cellulose (MCC) were used to analyze the difference between chemical and physical cellulose structures with and without encapsulation. Cellulose hydrogels were synthesized to encapsulate the bioactive compounds of the extracts. The synthesis hydrogel process is described in Figure 5.1:

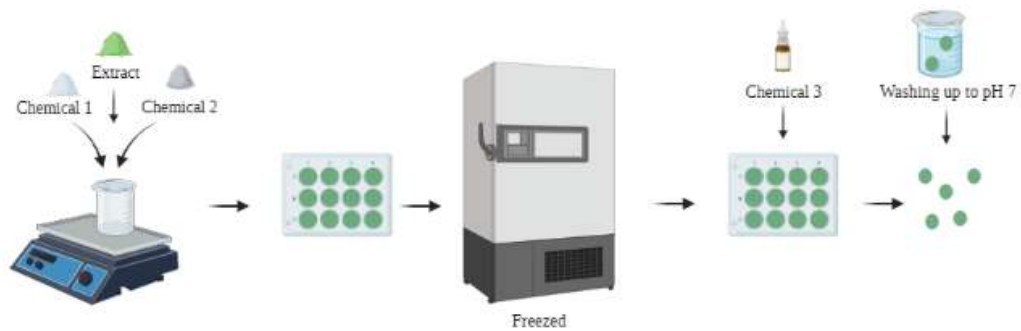


Figure 5.1: Synthesis of cellulose hydrogel with plants extracts

The hypothetical encapsulation of the extracts in the cellulose hydrogel is illustrated in the figure 5.2.:

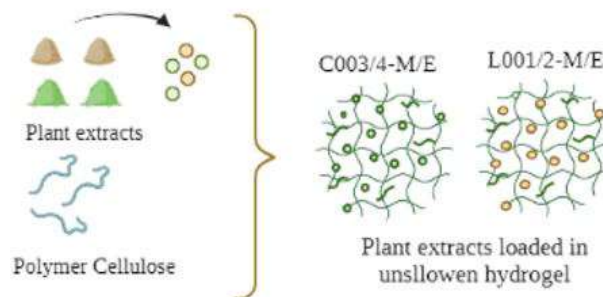


Figure 5.2: Extract loaded-hydrogels relative structure.

## 5.2.2 Fourier-Transform Infrared spectroscopy

### Samples preparation

Fourier-transform infrared (FT-IR) spectra were recorded using a Cary 630 Fourier Agilent spectrometer in the 4000–450  $\text{cm}^{-1}$  frequency range, at a resolution of 4  $\text{cm}^{-1}$  [68]. FT-IR spectroscopy of the lyophilized L001-M/NRC, L001-M/MCC, L002-E/NRC, L002-E/MCC, C003-M/NRC, C003-M//MCC, C004-E/NRC, and C004-E/MCC hydrogels were carried out compared with WE/NRC and WE/MCC samples, WE mean without extract.

### Results and discussion

Figures 5.3 and 5.4. the red line spectrum corresponds to WE/NRC and WE/MCC samples. The 3100–3600  $\text{cm}^{-1}$  peak corresponds to O-H stretching; meanwhile, the 2700–3000  $\text{cm}^{-1}$  peak refers to C-H stretching. Similarly, the peak near 1700  $\text{cm}^{-1}$  is related to

C=O stretching. Finally, the peak 900-1100  $\text{cm}^{-1}$  corresponds to the functional group C-O stretching  $\text{cm}^{-1}$  [69]. These functional groups are presented as NRC and MCC hydrogels without extract, but their difference lies in the higher intensity range between 900-1100  $\text{cm}^{-1}$  in the NRC hydrogels.

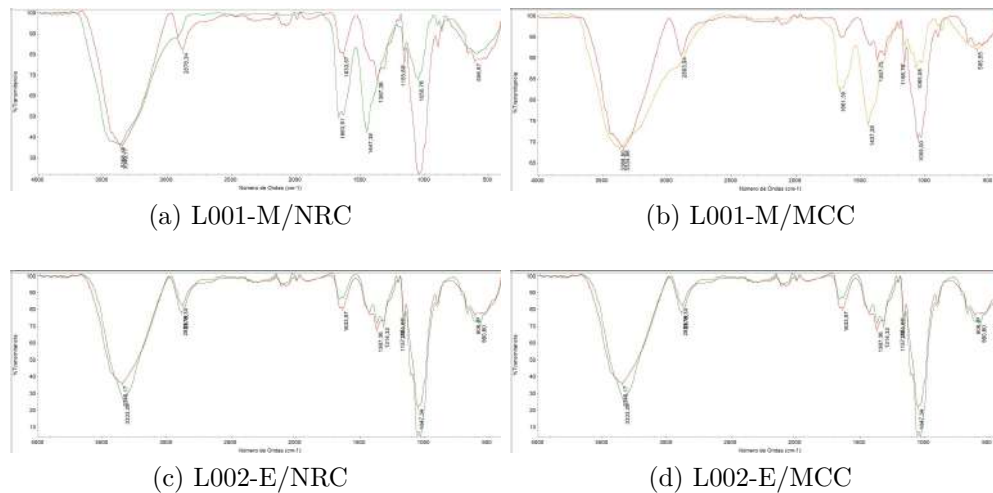


Figure 5.3: FT-IR Spectrum of plant extract (green line=spectrum with extract) compared with WE hydrogels (red line=spectrum without extract).

The characteristic peaks (green line) of L001-M in 1663.91  $\text{cm}^{-1}$  and 1447.38  $\text{cm}^{-1}$  for the NRC hydrogel type (a) (See Figure 5.3). Meanwhile, 1661.39  $\text{cm}^{-1}$  and 1437.28  $\text{cm}^{-1}$  peaks are visible in L001-M/MCC (b) hydrogels which are not present in the xerogel spectrum. Therefore, the spectrum of extract L002-E (c,d) needs to be repeated because the difference is not detected. The peaks of C003-M/NRC (e) are 1663.25  $\text{cm}^{-1}$  and 1445.41  $\text{cm}^{-1}$ , and C003-M/NRC (f) shows 1659.92  $\text{cm}^{-1}$  and 1438.76  $\text{cm}^{-1}$  (See Figure 5.4.). In addition, peaks 1629.44  $\text{cm}^{-1}$  and 1441.34  $\text{cm}^{-1}$  are also identified. Similarly, for C004-E/NRC (g) it is 1667.40  $\text{cm}^{-1}$  and 1460.56  $\text{cm}^{-1}$  for C004-E/MCC (h).

Evidence illustrated that the spectrum without extract hydrogels differs from the extract loaded hydrogel. The peak between 2700 – 3000  $\text{cm}^{-1}$  present in the without extract hydrogels of NRC and MCC type corresponds to the C-H stretching [69]. This peak is not visible in the hydrogels in the extracts, according to Figure 5.4. While the peak in the region 3300 – 3400  $\text{cm}^{-1}$  is related to the O-H stretching functional group in the WE/NRC and WE/MCC with strong absorption. This peak is visualized in both the hydrogels with and without extract. On the other hand, the 1600 – 1700  $\text{cm}^{-1}$  corresponds to C=O

stretching in the cellulose hydrogels. The % transmittance of this peak increases when the hydrogels with the extract. Finally, 1000 – 1100  $\text{cm}^{-1}$  wavelength corresponds to the C-O stretching peak, whose transmittance decreases when in hydrogels loaded with the extract.

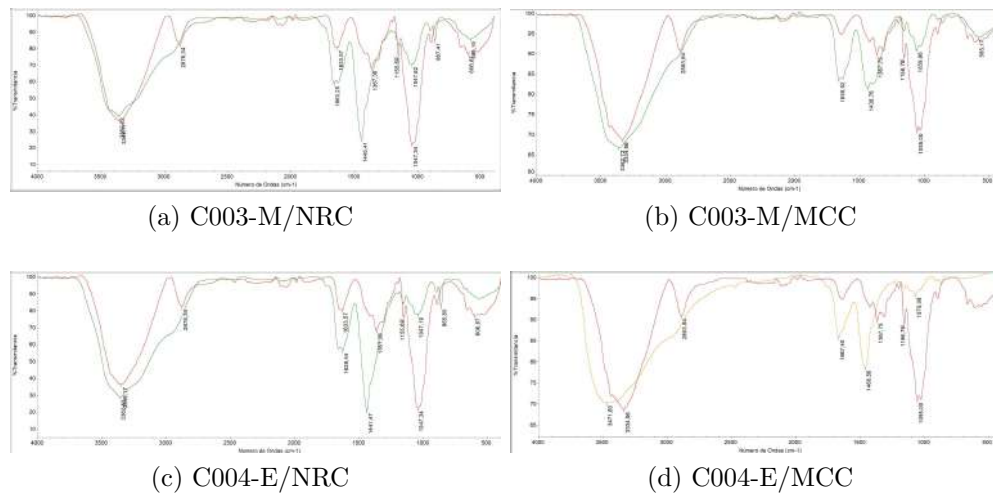


Figure 5.4: FT-IR Spectrum of plant extract (green line=spectrum with extract) compared with WE hydrogels (red line=spectrum without extract).

FT-IR could indicate that there is an optimal encapsulation of the extracts in the polymeric matrix of the hydrogel. It was evident that the encapsulation of the functional groups of the extracts differed from the without extract cellulose hydrogels. In addition, the Fourier-transform infrared characterization between the NRC and MCC cellulose types differed only in the peak % transmittance of the previously analyzed functional groups.

### 5.2.3 Surface morphology of hydrogel

The M205-C Stereo Microscope was used to analyze the morphology of the hydrogels and observe their surface in detail [70]. A magnification of 1.5 and 4 was used on L001-M/NRC, L001-M/MCC, L002-E/NRC, L002-E/MCC, C003-M/NRC, C003-M/MCC, C004-E/NRC, and C004-E/MCC, WE/NRC and WE/MCC for surface analysis. The three-dimensional structure of the cellulose hydrogel suffered swelling in the presence of an aqueous medium and the ability to retain different volumes of water. The hydrogels loaded with the extracts L001-M, L002-E, C003-M, and C004-E were hydrophilic and had a hyper-branched polymer network.

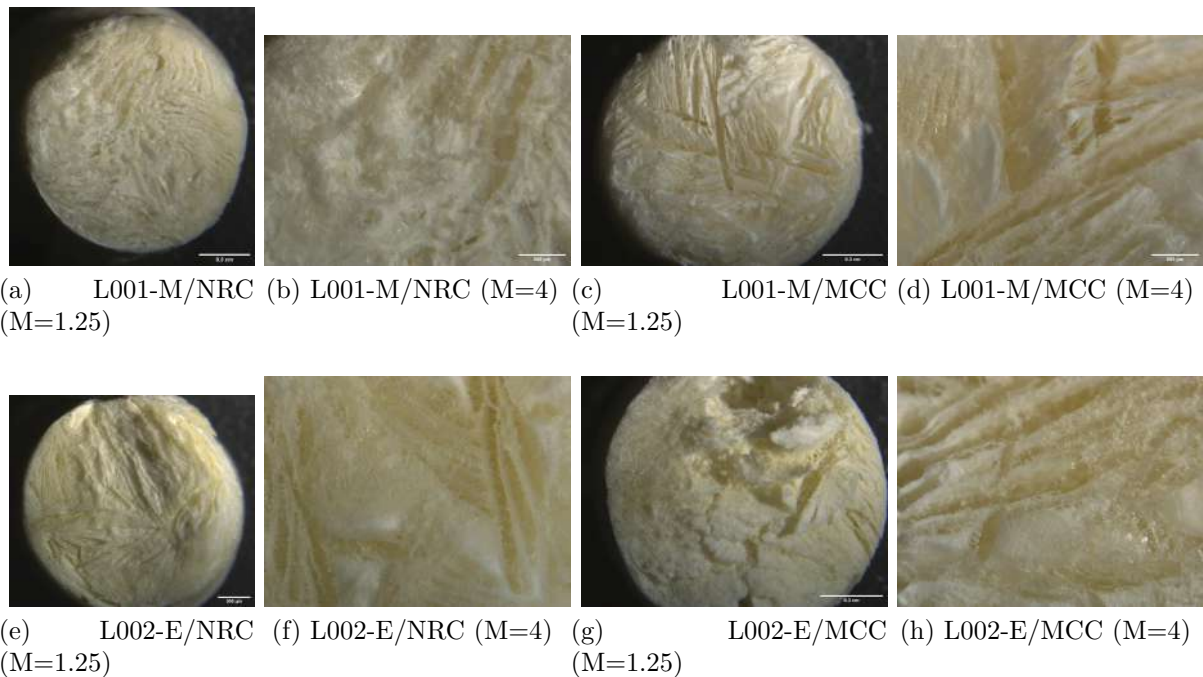


Figure 5.5: Surface morphology of plant extract loaded-hydrogel through stereoscope

In Figure 5.5, the yellowish surface color may suggest, at first glance, the encapsulation of the extracts in the NRC and MCC hydrogels. Through the stereoscope, it is visualized on the non-uniform surface. Indeed, samples showed a consistent structure.

Figure 5.6. corresponding to C003-M/MCC with different M, shows a more compact structure with the normal cellulose than the crystalline one. The extract particles were observed at a magnification of 4 since the sample is not 100% soluble in water. In contrast, these extract particles were not found in the C003-E cellulose type. It could be related to the water's 100% solubility or the sample chemical structure and the hydrogel components. Furthermore, the yellow color is more intense on the surface compared to the samples in Figure 5.5.

surface of the cellulose hydrogel between microcrystalline cellulose and cotton cellulose. The difference in color between the cellulose without the extracted compared to L001-M/NRC, L001-M/MCC, L002-E/NRC, L002-E/MCC, C003-M/NRC, C003-M//MCC, C004-E/NRC, and C004-E/MCC indicated encapsulation of extract compared to the WE/NRC and WE/MCC hydrogels. Unique features such as the surface morphology of the loaded hydrogels developed in this research may limit their potential biomedical applications. The

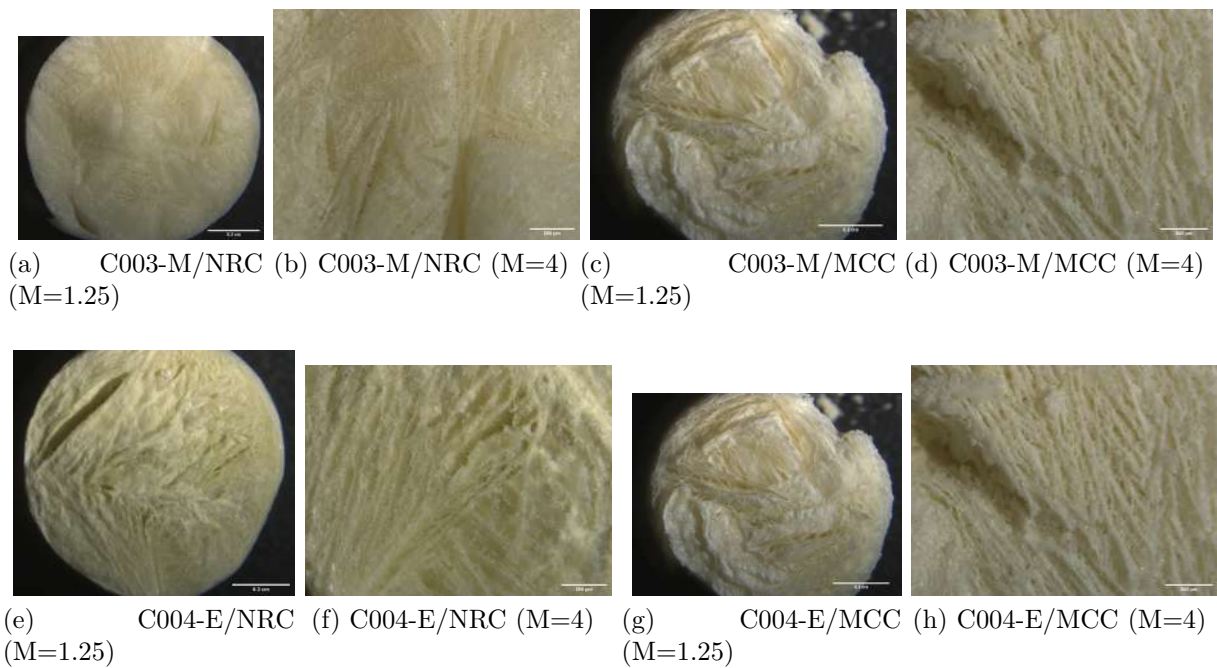


Figure 5.6: Surface morphology of plant extract loaded-hydrogel through stereoscope

physical integrity of the extract-loaded hydrogels could also be related to their mechanical strength, functionality, and adaptability [71].

### 5.3 Density and swelling of hydrogel

Cellulose hydrogel density was determined by the equation (10) based on the mass per unit volume, then hydrogels samples were weighed and dimensions calculated with the volume equation (11) [72]:

$$\rho = \frac{m}{V} \quad (10)$$

$$V = \pi * r^2 * h \quad (11)$$

where  $m$  means mass,  $V$  is the volume,  $r$  means radio and  $h$  is height.

Correspondingly, the swelling degree of hydrogel was studied in order to analyze the maximum level of liquid that can be absorbed depending on the degree of swelling. It used the phosphate buffer saline (PBS) adjusted to a pH of 7.4 at 37°C. The measure started

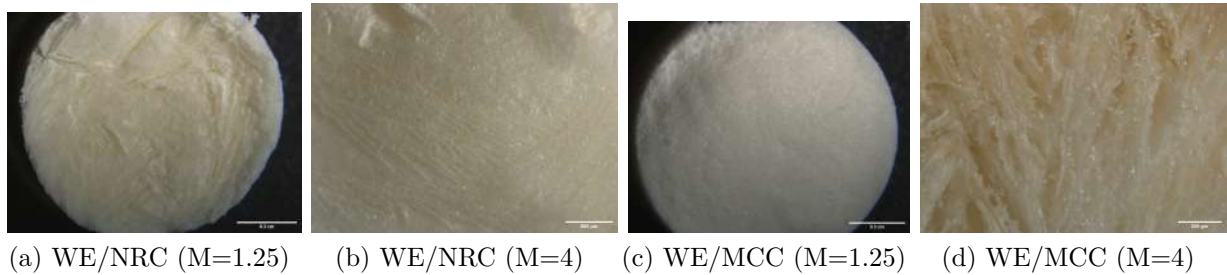


Figure 5.7: Surface morphology of plant extract through stereoscope

with a dried hydrogel and weight measure. Then, samples were immersed in PBS at 37°C and weighed at 0, 3, 6, 9, 12, 24, and 28 hours. The objective of this procedure is to study the absorption capacity.

The degree of swelling is calculated with the equation (12) [73]

$$\text{Degree of swelling} = \frac{m_s - m_d}{m_d} * 100 \quad (12)$$

where  $m_d$  corresponds to the weight of the dry hydrogel and  $m_s$  is the weight of the swollen hydrogel at a specific time.

### Results and discussion

The Table 5.1. along with the hydrogel density based on water density, the value of which is ( $0.9978g/cm^3$ ) at 4°C [74]. The reference literature reports values of  $1.028g/cm^3$  value density of microcrystalline cellulose and the cotton cellulose density corresponds to  $1.44g/cm^3$ . [75, 76].

For the experimental analysis, the density of the hydrogels including the extracts concentration of 2.5 mg/mL is higher than 1 mg/mL in both cellulose types (See Table 5.1.). Evidence illustrates that increasing the concentration of the extracts therefore increases the number of molecules stored in the three-dimensional matrix of the hydrogel.

Results demonstrated that the density of the loaded-hydrogel of MCC is higher than NRC. Also, the density of the hydrogels without the extracts (WE) is relatively higher, being  $1.054g/cm^3$  for NRC and  $1.208g/cm^3$  for MCC (See Table 5.1.). In the final analysis, hydrogels loaded with C003-M and C004-E extracts of each cellulose type showed higher density than their counterparts L001-M and L002-E. This suggests that phytochemical

Hydrogels	Plant extract concentration					
	1 mg/mL of extract			2.5 mg/mL		
	Volume (cm <sup>3</sup> )	Mass (g)	Density (g/cm <sup>3</sup> )	Volume (cm <sup>3</sup> )	Mass (g)	Density (g/cm <sup>3</sup> )
L001-M/NRC	1.135	0.850	0,749	1.272	0.970	0.763
L001-M/MCC	1.866	1.085	0.967	1.701	1,714	1,008
L002-E/NRC	1.155	0.994	0.861	1.344	1.206	0.897
L002-E/MCC	1.900	1.873	0.986	1.909	1.989	1.042
C003-M/NRC	1.128	0.853	0.756	1.005	0.874	0.869
C003-M//MCC	1.586	1.395	0.880	1.418	1.494	1.054
C004-E/NRC	1.021	0.900	0.881	1.135	1.029	0.906
C004-E//MCC	1.586	1,477	0.931	1.571	1.731	1.102
WE/NRC	1.362	1.435	1.054	1.362	1.435	1.054
WE/MCC	1.589	1.920	1.208	1.589	1.920	1.208

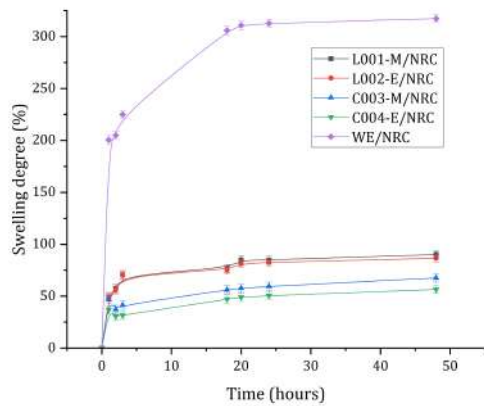
NRC: Cotton cellulose; MCC: Microcrystalline cellulose; WE: without extract

Table 5.1: Cellulose hydrogel density.

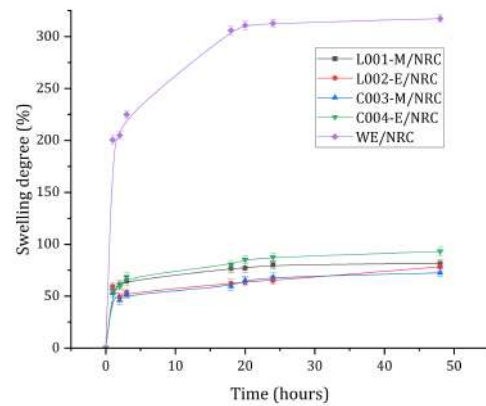
compounds from the second plant could modify the density value. The density of hydrogel is related to the swelling ratio of hydrogels and other mechanical properties. Density is an influential factor in the dimensional change, and the release patterns of extract from these carriers [77]. After analysis, the loaded-hydrogel swelling hydrogel study is important for future biomedical applications.

The degree of diffusion of the extract components through the hydrogel is relevant for biomedical used extract delivery system [78]. The influence of the extract concentration on the swelling ratio of cellulose hydrogel in PBS at pH 7.4 was shown in Figure 5.8. The WE/NRC and WE/MCC exhibited a high equilibrium swelling ratio, indicating the hydrogels were superabsorbent without extract hydrogels. The amount of water stored by the hydrogels depends on the pH of the medium and the ionic strength characterized by the ionic groups, and the level of crosslinking of the polymer network [79]

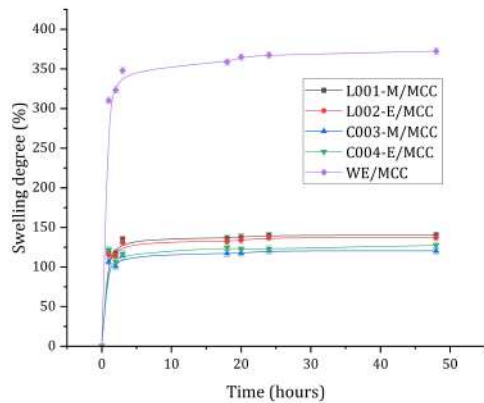
The results showed significant differences between WE/NRC and WE/MCC hydrogels and loaded-hydrogels containing the extracts at different concentrations (See Figure 5.8.). Although the chemical components of the L001-M/NRC and L001-E/NRC extracts are similar, the swelling degree was significantly different, even at 1 mg/mL. The same statistical analysis was founded when L001-M/NRC and L001-E/NRC were compared at 2.5 mg/mL. It indicated that the swelling degree is affected by the solvent from which the extract is obtained. In addition, the percentage of swelling degree decreased when the



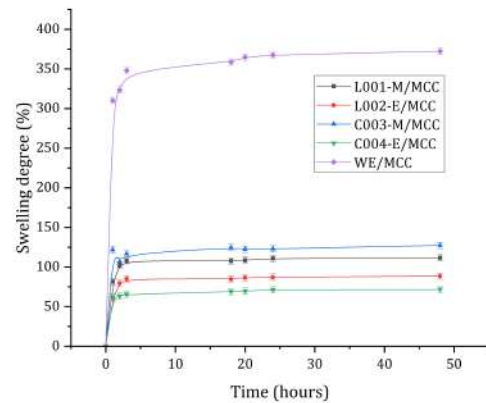
(a) NRC hydrogel at 1 mg/mL



(b) NRC hydrogel at 2.5 mg/mL



(c) MCC hydrogel at 1 mg/mL



(d) MCC hydrogel at 2.5 mg/mL

Figure 5.8: Degree of swelling of NRC and MCC hydrogels type in PBS solution.

concentration of the extract L001-m and L002-E was increased. It may be due to the increase of bioactive compounds in the three-dimensional matrix of the hydrogel. The same statistical analysis was used to compare the L001-M/MCC and L001-E/MCC, having similar statistical results for loaded-hydrogel at 1 mg/mL and 2mg/mL. Furthermore, it was observed that swelling loaded-hydrogels corresponded to the 25 – 85% range, while the hydrogel without extract in NRC and MCC hydrogel showed a swelling degree of 300%.

Analyzing the C003-M/NRC and C004-E/NRC swelling degree, there is a significant difference in swelling percentage at 1 mg/mL and 2.5 mg/mL extract concentration. The evidence illustrated that the swelling capacity increased as the C003-M and C004-E content incremented. Whereas the C003-M/MCC and C004-E/MCC hydrogels maintain a

similar swelling degree profile as the extract concentration increases, statistically, there is a significant difference when the hydrogels are compared at the concentration of 1 mg/mL and 2.5 mg/mL.

Results showed optimal release of extracts under conditions of a dynamic pH-based study with phosphate buffer solutions (pH 7.4). The microcrystalline cellulose demonstrated a higher degree of swelling than NRC cellulose hydrogels. The WE/MCC was swelling up to 375%. Also, the extract-loaded MCC hydrogel showed a higher swelling value than NRC samples. The swelling values of the hydrogel increased considerably in the first 5 hours, followed by augmenting steeply up to 24 hours. Thus, the degree of swelling is inversely proportional to the concentration of the extract [80] for L001-M and L002-E. The swelling had different behavior for C003-M and C003-E loaded-hydrogel. Hydrogels with methanol extracts show better swelling than ethanolic extracts. Finally, the swelling process depends on the extract concentration because it could affect the rate and speed of release.

## 5.4 Loaded-hydrogel release profiles

Extract-loaded hydrogel L001-M/NRC, L001-M/MCC, L002-E/NRC, L002-E/MCC, C003-M/NRC, C003-M//MCC, C004-E/NRC, and C004-E//MCC at a concentration of 1mg/mL, also xerogel WE/NRC and WE/MCC were dried at 45 °C. Then cellulose hydrogels were immersed in 4 mL of phosphate buffer pH 7.4. The experiment was carried out in the MaxQ™ 4450 Benchtop Orbital Shaker at 25 revolutions per minute for 72 hours at 37 °C. The samples were replicated by triplicate, and the weight variation of the hydrogels with an approximate value of 500 mg and 850 mg, respectively.

NanoDrop™ 2000 Spectrophotometers measured the amount of extract released through periodic measurements applying spectrophotometry. A 5 uL aliquot was taken from the buffer where the hydrogels were immersed. The absorbance values correlating to the release profiles were fitted to the following linear regression equation (13).

$$\frac{M_t}{M_\infty} = K * t^n \quad (13)$$

where  $\frac{M_t}{M_\infty}$  the ratio of extract released and t corresponding to the time.

The equation (13) corresponding to Korsmeyer-Peppas mathematica model was based on the drug released from the cellulose hydrogel literature reference [81, 82]. The absorbance of the extracts at the following wavelengths was recorded according to Table 5.2. values.

Sample	Maximum peak (nm)
L001-M	$\lambda = 295$
L002-E	$\lambda = 285$
C003-M	$\lambda = 410$
C004-E	$\lambda = 415$

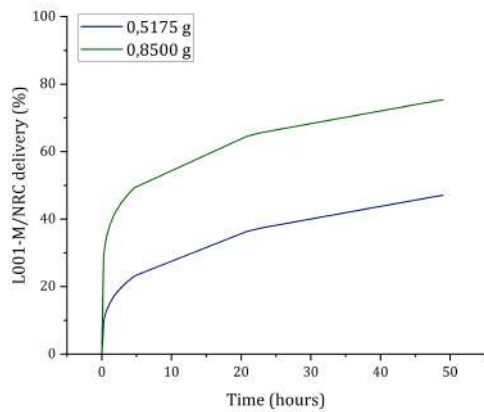
Table 5.2: Maximum peak based on UV-Vis spectra of plants extracts

### Results and discussion

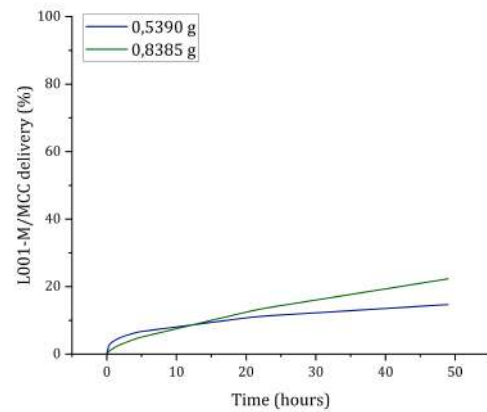
The experimental result of the *in vitro* extract released from the cotton cellulose and crystalline cellulose in PBS at a pH of 7.4 is shown in Figures 5.9 and 5.10. The release studies were conducted by keeping two different hydrogels weights. After fitting experimental data with the Korsmeyer-Peppas equation (13), it was determined that the increased extract amount released is proportional to the hydrogel weight. However, a considerable difference between the release achieved by cotton cellulose and microcrystalline cellulose could be influenced by the degree of crosslinking of the polymers and the physical properties [83]. The extract's release occurred owing to the pore size increase of the matrix network due to swelling loaded-hydrogel beads [80] affecting the extract release. Extract release profiles differ between NRC and MCC loaded-hydrogel types.

Figure 5.9. indicated that L001-M/NRC and L002-E/NRC demonstrate an extract releasing up to 80%. Meanwhile, extract release in L001-M/MCC, and L002-E/MCC only achieved less than 30% in both hydrogel types. Moreover, the L001-M/NRC and L002-E/NRC samples are significantly different in other terms, demonstrating that the release profiles are independent of the amount of hydrogel used. In contrast, the L001-M/MCC released profile was not different scientifically at 0.5175g and 0.8500g. in view of this, the release of the L001-M extract shows the same trend in percent release. Nevertheless, L002-E/MCC did not show a significant difference at 95%.

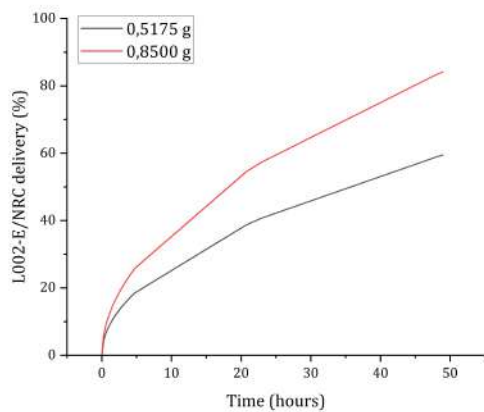
Results in the Figure 5.10. are related to the delivery percentage of C003-M/NRC, C003-M/MCC, C004-M/NRC, and C004-E/MCC samples. C003-M and C004-E extract



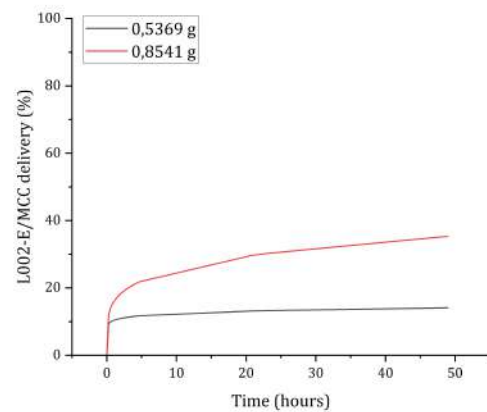
(a) L001-M/NRC hydrogel delivery



(b) L001-M/MCC hydrogel delivery



(c) L002-E/NRC hydrogel delivery

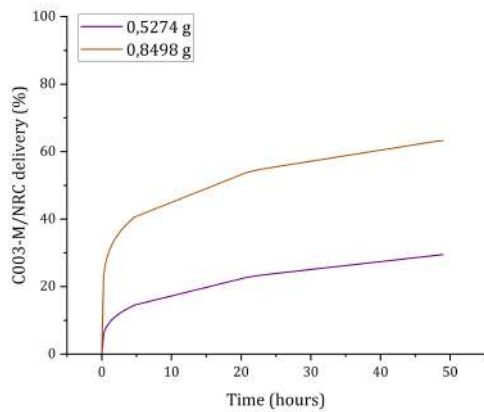


(d) L002-E/MCC hydrogel delivery

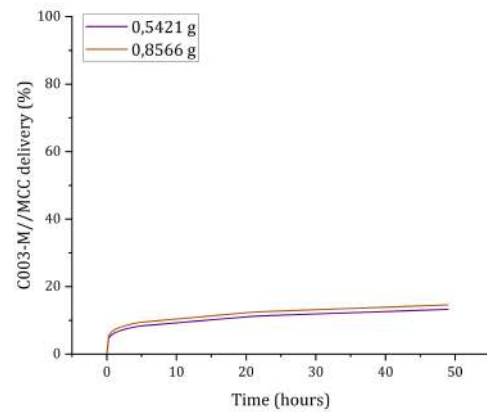
Figure 5.9: Plant extracts releasing data from the NRC and MCC loaded-hydrogel in PBS pH (7.4)

releasing were until 60% in NRC hydrogel type; at the same time, releasing reached 30% for MCC samples. Statistically, the data showed a significant difference between hydrogel size and the amount of extract released for C003-M/NRC and C004-E/. In comparison, the delivery of C003-M/MCC hydrogel showed a significant difference. The delivery of C004-E/MCC hydrogel was not statistically different, so the hydrogel weight does not influence the liberation of C004-E extract from MCC hydrogel.

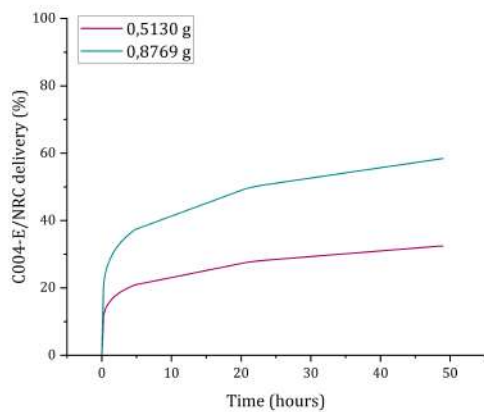
The release profile can be influenced by the extract's solubility and the hydrogel's size or shape, which directly influence the data's model fit of the data [28]. Through the results of the release profiles, the dissociation of the trapped particles through the mechanism of



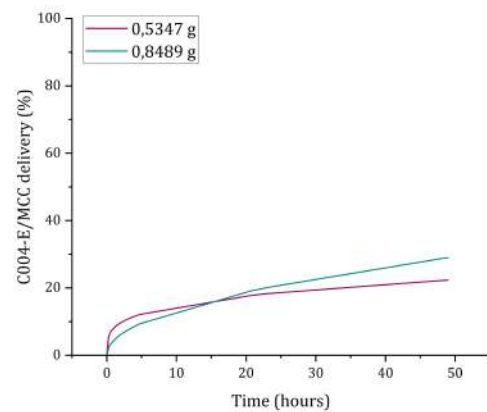
(a) C003-M/NRC hydrogel delivery



(b) C003-M/MCC hydrogel delivery



(c) C004-E/NRC hydrogel delivery



(d) C004-E/MCC hydrogel delivery

Figure 5.10: Plant extracts releasing data from the NRC and MCC loaded-hydrogel in PBS pH (7.4)

diffusion through the hydrogel was verified.

## 5.5 Biological activity of loaded-hydrogel

The antibacterial activity of the loaded-hydrogel with the plant extract using the Gram-negative bacteria (*E. coli*) called DH5- $\alpha$  because the antibacterial activity of the extract alone was found in this cell line. For the inoculums preparation, in 2ml of Luria Bertani agar, 25 ul of the DH5- $\alpha$  bacteria were added and then incubated at 37 °C with 160 revolutions per minute for 24 hours.

### Hydrogel preparation

The Kirby–Bauer (KB) method was applied in the L001-M/NRC, L001-M/MCC, L002-E/NRC, and L002-E/MCC to evaluate the antimicrobial activity of WE/NRC and WE/MCC loaded-hydrogel against DH5- $\alpha$  [84]. For loaded-hydrogel testing, disc-shaped samples were prepared with a height of 0.7 cm and a diameter of 1.9 cm. The hydrogel loaded with the extract was washed until it reached a pH close to 7. To the medium was added a volume of 300 ul of inoculums preparation. The hydrogel was placed over Luria Bertani Agar solid in sterile Petri dishes. After 24 h of incubation at 37 °C, the inhibition halo was measured.

### Results and discussion

The inhibition halo reported the antibacterial activity of cellulose hydrogel. The positive control was kanamycin as a commercial antibiotic at 5 mg/mL, while the extract concentration of hydrogel was 2.5 mg/mL for L001-M and L002-E. Figure 5.11 showed the inhibition halo of extract loaded-hydrogel after 24 hours of incubation. Then, halo forming on the microcrystalline cellulose hydrogels demonstrated the antibacterial activity of the hydrogels loaded with the plant extract against DH5- $\alpha$  cell line [85]. These results are consistent with the well-known antibacterial activity of kanamycin [86]. In contrast, the WE/NRC and WE/MCC-loaded hydrogel had no antibacterial activity as was expected. Also, it was evident that average cell growth in the negative control section (See Table 5.3.).

Sample	Hydrogel type		
	/NRC	/MCC	Positive C.
L001-M/	NA	3.17236	3.43003
L002-E/	NA	2.93102	3.49799
WE/	NA	NA	3.52462

Table 5.3: Antibacterial activity of extract loaded-hydrogel, NA = non active

The difference in antibacterial activity detected in the MCC-type hydrogels compared to the NRC type may be related to the amount of extract released by the hydrogel and, therefore, to the swelling rate ratio. The L001-M/MCC hydrogel produces an inhibition halo of 3,172 cm for DH5- $\alpha$ . Meanwhile, the L002-E/MCC formed an inhibition halo of 2,931 cm for the same cell line. In particular, the positive control (kanamycin) shows an inhibition halo of 3,430 for L001-M/MCC and 3,498 for L002-E/MCC. Through t-Test was determined that the L001-M/MCC and L002-E/MCC are not significantly different, i.e.,

there is no difference in the antibacterial activity of the extract-loaded-hydrogel. Similarly, compared to the biological activity recorded by the extract-loaded hydrogel of type MCC compared to its positive control, at a significance level of 95%, it is determined that they are not significantly different. Therefore, the 2.5 mg/mL extract and 5 mg/mL of kanamycin delivered from the microcrystalline cellulose hydrogels showed the same antibacterial effect.

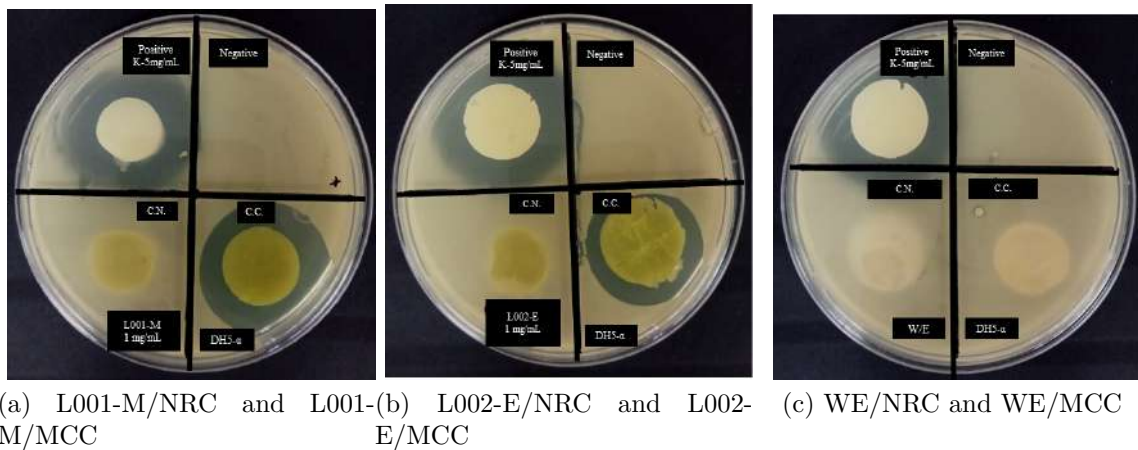


Figure 5.11: Antibacterial activity of the extract-loaded hydrogels.

The ability of L001-M/MCC and L002-E/MCC hydrogel to inhibit the growth of bacteria could be due to one specific presence of a secondary metabolite or the synergy [12]. The diverse chemical groups interact with bacterial membranes due to hydrophobic-hydrophobic interactions, thus enhancing cell membrane outgrowth and harming the structure of bacterial cells [15]. Finally, the positive antibacterial result of extract loaded-hydrogel could be useful for cellulose-based biomedical devices.



# Chapter 6

## Conclusions

### Extract synthesis and characterization

It was determined that the natural extracts L001-M, L002-E, C003-M, and C004-M were successfully obtained through methanol and ethanol extractions with positive results in the *in vitro* studies of antibacterial, antioxidant, and anti-inflammatory activity. In addition, the components of the extracts were encapsulated in two types of cellulose hydrogels. The characterization results, swelling, release profile, and biological activity suggest their potential application as a controlled release system of natural compounds.

The outcomes provide insight that the synthesis and characterization of the four extracts allowed the qualitative identification of various secondary metabolites with possible bioactive interest, making the used species plants good candidates for drug development.

- The phytochemical profile of plant extracts showed that the extraction solvent influences the secondary metabolites obtained, principally alkaloids, coumarins, lactones, terpenes, flavonoids, phenols, tannins, and quinones. TLC also demonstrated the presence of this complexity of functional groups.
- The FT-IR and UV-Vis spectra supported as evidence the presence of previously identified functional groups in the phytochemical screening.

Biological activity results may suggest the promising medical use of plant extracts for pharmacological applications due to their ability to break the membrane of cell lines, could be a source of natural antioxidants, and ability to prevent the breakdown of the erythrocyte membrane.

- The L001-M and L002-E extract showed antimicrobial activity against *E. coli* DH5- $\alpha$ . L001-M extract presented a more efficient relative antibacterial activity through time compared with L002-E.
- The antioxidant TAC and FRP assays indicated that L001-M extract has a strong antioxidant capacity.
- High antioxidant and antibacterial activity were reported when concentration increased. Results demonstrated that the best extraction solvent for antioxidant molecules is methanol.
- The C004-E extract showed a higher anti-inflammatory response.

The hydrogel formulation allowed the encapsulation conditions of the bioactive compounds of plant extracts to be tested through the characterization of the loaded hydrogels as well as the swelling, release, and antibacterial activity assays and their potential biomedical application. There was an effective enclosure of natural extracts in cotton and microcrystalline cellulose hydrogels.

- The concentration of 1 mg/mL and 2.5 mg/mL optimize the desired therapeutic effect while preserving the mechanical and kinetic properties of the hydrogel.
- Evidence illustrated the interaction of the hydrogel with the extracts supported by the FT-IR spectra. The morphology visualized exhibited a crumpled surface in the hydrogel.
- The NRC cellulose type is a more suitable material for developing these hydrogels due to its better release capacity.
- L001-M/MCC and L002-E/MCC loaded-hydrogel inhibited the growth of the DH5- $\alpha$  cell line.

### **Future work**

The limitations of analysis and characterization developed in the research study have indicated the following areas as recommendations for further work.

- Develop chemical analysis tools for secondary plant metabolites such as high-performance liquid chromatography, nuclear magnetic resonance spectroscopy, and liquid chromatography mass spectrometry.
- Perform *in vitro* antibacterial activity assays with gram-positive cells and other antioxidant activity assays such as DPPH, ABTS, and CUPRAC.
- Characterize the hydrogels loaded with the extracts through a scanning electron microscope for visualization of pores and morphology, perform other studies such as differential scanning calorimetry, and explore the potential pharmacological applications of the same.



# Bibliography

- [1] D. T. D. Nguyen, M. T. Vo, C. T. Truong, D. H. Nguyen, T. A. Nguyen Thi, T. N. Huynh Truc, N. T. Viet, and M. H. Vo Do, “Oleoresin for Pharmaceutical Applications,” *Evid Based Complement Alternat Med*, vol. 2021, p. 8229607, 2021.
- [2] R. M. Perez, “Anti-inflammatory activity of compounds isolated from plants,” *ScientificWorldJournal*, vol. 1, pp. 713–784, Nov 2001.
- [3] W. X. Waresindo, H. R. Luthfianti, D. Edikresnha, T. Suciati, F. A. Noor, and K. Khairurrijal, “A freeze–thaw pva hydrogel loaded with guava leaf extract: Physical and antibacterial properties,” Sep 2021. [Online]. Available: <https://pubs.rsc.org/en/content/articlelanding/2021/ra/d1ra04092h#!>
- [4] A. Mansoori, S. T. T. Singh, N. and Dubey, N. Alkan, S. Das, and A. Kumar, “Phytochemical Characterization and Assessment of Crude Extracts From *Lantana camara* L. for Antioxidant and Antimicrobial Activity,” *Frontiers in Agronomy*, vol. 2, no. 1, p. 582268, 2020.
- [5] A. Altemimi, N. Lakhssassi, A. Baharlouei, D. G. Watson, and D. A. Lightfoot, “Phytochemicals: Extraction, Isolation, and Identification of Bioactive Compounds from Plant Extracts,” *Plants (Basel)*, vol. 6, no. 4, Sep 2017.
- [6] M. W. Wang, X. Hao, and K. Chen, “Biological screening of natural products and drug innovation in China,” *Philos Trans R Soc Lond B Biol Sci*, vol. 362, no. 1482, pp. 1093–1105, Jun 2007.
- [7] E. S. Teoh, “Secondary metabolites of plants,” *Medicinal Orchids of Asia*, p. 59–73, 2016.

- [8] A. M. L. Seca and D. C. G. A. Pinto, “Biological Potential and Medical Use of Secondary Metabolites,” *Medicines (Basel)*, vol. 6, no. 2, Jun 2019.
- [9] J. Reichling, “Plant-microbe interactions and secondary metabolites with antibacterial, antifungal and antiviral properties,” *Functions and Biotechnology of Plant Secondary Metabolites*, p. 214–347, 2010.
- [10] S. Goyal, C. Lambert, S. Cluzet, J. M. Mérillon, and K. G. Ramawat, “Secondary metabolites and plant defence,” *Plant Defence: Biological Control*, p. 109–138, 2011.
- [11] R. B. Karina, “Extracción y caracterización de metabolitos secundarios (polifenoles y flavonoides) obtenidos a partir de pujín (*hesperomeles ferruginea*) planta nativa del cerro teligote,” Aug 2020. [Online]. Available: <https://repositorio.uta.edu.ec/bitstream/123456789/32124/1/AL%20774.pdf>
- [12] L. Othman, A. Sleiman, and R. M. Abdel-Massih, “Antimicrobial activity of polyphenols and alkaloids in middle eastern plants,” *Frontiers in Microbiology*, vol. 10, 2019.
- [13] M. M. Cowan, “Plant products as antimicrobial agents,” *Clinical Microbiology Reviews*, vol. 12, no. 4, p. 564–582, 1999.
- [14] B. Khameneh, M. Iranshahy, V. Soheili, and B. Fazly Bazzaz, “Review on plant antimicrobials: A mechanistic viewpoint,” *Antimicrobial Resistance amp; Infection Control*, vol. 8, no. 1, 2019.
- [15] F. D. Gonelimali, J. Lin, W. Miao, J. Xuan, F. Charles, M. Chen, and S. R. Hatab, “Antimicrobial Properties and Mechanism of Action of Some Plant Extracts Against Food Pathogens and Spoilage Microorganisms,” *Front Microbiol*, vol. 9, p. 1639, 2018.
- [16] B. Kot, K. Kwiatek, J. Janiuk, M. Witeska, and A. Pekala-Safińska, “Species Isolated from Fish,” *Pathogens*, vol. 8, no. 3, Sep 2019.
- [17] G. Llauradó Maury, D. Méndez Rodríguez, S. Hendrix, J. C. Escalona Arranz, Y. Fung Boix, A. O. Pacheco, J. García Díaz, H. J. Morris-Quevedo, A. Ferrer Dubois,

- E. I. Aleman, and et al., “Antioxidants in plants: A valorization potential emphasizing the need for the conservation of plant biodiversity in cuba,” *Antioxidants*, vol. 9, no. 11, p. 1048, 2020.
- [18] M. Ji, X. Gong, X. Li, C. Wang, and M. Li, “Advanced research on the antioxidant activity and mechanism of polyphenols from hippophae species—a review,” *Molecules*, vol. 25, no. 4, p. 917, 2020.
- [19] A. M. Pisoschi, A. Pop, C. Cimpeanu, and G. Predoi, “Antioxidant capacity determination in plants and plant-derived products: A review,” *Oxidative Medicine and Cellular Longevity*, vol. 2016, p. 1–36, 2016.
- [20] D. M. Kasote, S. S. Katyare, M. V. Hegde, and H. Bae, “Significance of antioxidant potential of plants and its relevance to therapeutic applications,” *International Journal of Biological Sciences*, vol. 11, no. 8, p. 982–991, 2015.
- [21] M. N. Alam, N. J. Bristi, and M. Rafiquzzaman, “Review on in vivo and in vitro methods evaluation of antioxidant activity,” *Saudi Pharm J*, vol. 21, no. 2, pp. 143–152, Apr 2013.
- [22] A. Blainski, G. Lopes, and J. de Mello, “Application and analysis of the folin-ciocalteu method for the determination of the total phenolic content from limonium brasiliense l.” *Molecules*, vol. 18, no. 6, p. 6852–6865, 2013.
- [23] Q. Sun, J. Zhu, F. Cao, and F. Chen, “Anti-inflammatory properties of extracts from chimonanthus nitens oliv. leaf,” *PLOS ONE*, vol. 12, no. 7, 2017.
- [24] C. d. Nunes, M. Barreto Arantes, S. Menezes de Faria Pereira, L. Leandro da Cruz, M. de Souza Passos, L. Pereira de Moraes, I. J. Vieira, and D. Barros de Oliveira, “Plants as sources of anti-inflammatory agents,” *Molecules*, vol. 25, no. 16, p. 3726, 2020.
- [25] K. Fylaktakidou, D. Hadjipavlou-Litina, K. Litinas, and D. Nicolaidis, “Natural and synthetic coumarin derivatives with anti-inflammatory / antioxidant activities,” *Current Pharmaceutical Design*, vol. 10, no. 30, p. 3813–3833, 2004.

- [26] N. Micale, A. Citarella, M. S. Molonia, A. Speciale, F. Cimino, A. Saija, and M. Cristani, “Hydrogels for the Delivery of Plant-Derived (Poly)Phenols,” *Molecules*, vol. 25, no. 14, Jul 2020.
- [27] A. Kyriakoudi, E. Spanidi, I. Mourtzinos, and K. Gardikis, “Innovative delivery systems loaded with plant bioactive ingredients: Formulation approaches and applications,” *Plants*, vol. 10, no. 6, p. 1238, 2021.
- [28] W.-F. Lai and A. L. Rogach, “Hydrogel-based materials for delivery of herbal medicines,” *ACS Applied Materials amp; Interfaces*, vol. 9, no. 13, p. 11309–11320, 2017.
- [29] T. Dhanani, S. Shah, N. Gajbhiye, and S. Kumar, “Effect of extraction methods on yield, phytochemical constituents and antioxidant activity of withania somnifera,” *Arabian Journal of Chemistry*, vol. 10, 2017.
- [30] E. Iqbal, K. A. Salim, and L. B. Lim, “Phytochemical screening, total phenolics and antioxidant activities of bark and leaf extracts of goniotalamus velutinus (airy shaw) from brunei darussalam,” *Journal of King Saud University - Science*, vol. 27, no. 3, p. 224–232, 2015.
- [31] M. A. Gacem, A. Telli, H. Gacem, and A. Ould-El-Hadj-Khelil, “Phytochemical screening, antifungal and antioxidant activities of three medicinal plants from algerian steppe and sahara (preliminary screening studies),” *SN Applied Sciences*, vol. 1, no. 12, 2019.
- [32] M. S. Auwal, S. Saka, I. A. Mairiga, K. A. Sanda, A. Shuaibu, and A. Ibrahim, “Preliminary phytochemical and elemental analysis of aqueous and fractionated pod extracts of *Acacia nilotica* (Thorn mimosa),” *Vet Res Forum*, vol. 5, no. 2, pp. 95–100, 2014.
- [33] R. María, M. Shirley, C. Xavier, S. Jaime, V. David, S. Rosa, and D. Jodie, “Preliminary phytochemical screening, total phenolic content and antibacterial activity of thirteen native species from guayas province ecuador,” *Journal of King Saud University - Science*, vol. 30, no. 4, p. 500–505, 2018.

- [34] F. E. Amrati, M. Bourhia, M. Slighoua, S. Ibneoussa, A. Bari, R. Ullah, A. Amagh-nouje, F. Di Cristo, M. El Mzibri, A. Calarco, L. Benbacer, and D. Bousta, "Extract and Its Bioactive Compound Classes," *Evid Based Complement Alternat Med*, vol. 2020, p. 8409718, 2020.
- [35] D. Tungmunnithum, A. Thongboonyou, A. Pholboon, and A. Yangsabai, "Flavonoids and Other Phenolic Compounds from Medicinal Plants for Pharmaceutical and Medical Aspects: An Overview," *Medicines (Basel)*, vol. 5, no. 3, Aug 2018.
- [36] N. Babbar, H. S. Oberoi, S. K. Sandhu, and V. K. Bhargav, "Influence of different solvents in extraction of phenolic compounds from vegetable residues and their evaluation as natural sources of antioxidants," *J Food Sci Technol*, vol. 51, no. 10, pp. 2568–2575, Oct 2014.
- [37] M. Rajani, N. Shrivastava, and M. N. Ravishankara, "A rapid method for isolation of andrographolide from andrographis paniculata nees (kalmegh)," *Pharm Biol*, vol. 38, no. 3, pp. 204–209, 2000.
- [38] I. A. Kagan and M. D. Flythe, "Thin-layer chromatographic (TLC) separations and bioassays of plant extracts to identify antimicrobial compounds," *J Vis Exp*, no. 85, Mar 2014.
- [39] W. Parys, M. Dołowy, and A. Pyka-Pajak, "Significance of chromatographic techniques in pharmaceutical analysis," *Processes*, vol. 10, no. 1, p. 172, 2022.
- [40] A. R. Abubakar and M. Haque, "Preparation of Medicinal Plants: Basic Extraction and Fractionation Procedures for Experimental Purposes," *J Pharm Bioallied Sci*, vol. 12, no. 1, pp. 1–10, 2020.
- [41] S. Donkor, C. Larbie, G. Komlaga, and B. O. Emikpe, "Phytochemical, antimicrobial, and antioxidant profiles of *Duranta erecta* L. Parts," *Biochem Res Int*, vol. 2019, p. 8731595, 2019.
- [42] P. Jain, A. Soni, P. Jain, and J. Bhawsar, "Phytochemical analysis of mentha spicata plant extract using uv-vis, ftir and gc/ms technique," *Journal of Chemical and Pharmaceutical Research*, vol. 2016, pp. 1–6, 02 2016.

- [43] R. A. Pratiwi and A. B. Nandiyanto, “How to read and interpret uv-vis spectrophotometric results in determining the structure of chemical compounds,” *Indonesian Journal of Educational Research and Technology*, vol. 2, no. 1, p. 1–20, 2022.
- [44] X. E. Mabasa, L. M. Mathomu, N. E. Madala, E. M. Musie, and M. T. Sigidi, 2021.
- [45] S. Sravan Kumar, P. Manoj, and P. Giridhar, “Fourier transform infrared spectroscopy (FTIR) analysis, chlorophyll content and antioxidant properties of native and defatted foliage of green leafy vegetables,” *J Food Sci Technol*, vol. 52, no. 12, pp. 8131–8139, Dec 2015.
- [46] A. Brangule, R. Šukele, and D. Bandere, “Herbal medicine characterization perspectives using advanced ftir sample techniques – diffuse reflectance (drift) and photoacoustic spectroscopy (pas),” *Frontiers in Plant Science*, vol. 11, 2020.
- [47] S. Agatonovic-Kustrin, E. Doyle, V. Gegechkori, and D. W. Morton, “High-performance thin-layer chromatography linked with (bio)assays and FTIR-ATR spectroscopy as a method for discovery and quantification of bioactive components in native Australian plants,” *J Pharm Biomed Anal*, vol. 184, p. 113208, May 2020.
- [48] Y. M. Reddy, S. P. J. Kumar, K. V. Saritha, P. Gopal, T. M. Reddy, and J. Simal-Gandara, “Ait. by LC-MS/MS Analysis and Evaluation of Its Antioxidant and Antimicrobial Activity,” *Plants (Basel)*, vol. 10, no. 3, Mar 2021.
- [49] A. A. Mostafa, A. A. Al-Askar, K. S. Almaary, T. M. Dawoud, E. N. Sholkamy, and M. M. Bakri, “Antimicrobial activity of some plant extracts against bacterial strains causing food poisoning diseases,” *Saudi Journal of Biological Sciences*, vol. 25, no. 2, p. 361–366, 2018.
- [50] J. L. Donay, P. Fernandes, P. H. Lagrange, and J. L. Herrmann, “Evaluation of the inoculation procedure using a 0.25 McFarland standard for the BD Phoenix automated microbiology system,” *J Clin Microbiol*, vol. 45, no. 12, pp. 4088–4089, Dec 2007.
- [51] S. Razmavar, M. A. Abdulla, S. B. Ismail, and P. Hassandarvish, “Antibacterial activity of leaf extracts of *Baccharis frutescens* against methicillin-resistant *Staphylococcus aureus*,” *BioMed Research International*, vol. 2014, p. 1–5, 2014.

- [52] L. J. Bessa, P. Fazii, M. Di Giulio, and L. Cellini, “Bacterial isolates from infected wounds and their antibiotic susceptibility pattern: some remarks about wound infection,” *Int Wound J*, vol. 12, no. 1, pp. 47–52, Feb 2015.
- [53] K. I. Udekwu, N. Parrish, P. Ankomah, F. Baquero, and B. R. Levin, “Functional relationship between bacterial cell density and the efficacy of antibiotics,” *J Antimicrob Chemother*, vol. 63, no. 4, pp. 745–757, Apr 2009.
- [54] M. Singhal, A. Paul, and H. P. Singh, “Synthesis and reducing power assay of methyl semicarbazone derivatives,” *Journal of Saudi Chemical Society*, vol. 18, no. 2, p. 121–127, 2014.
- [55] M. El Jemli, R. Kamal, I. Marmouzi, A. Zerrouki, Y. Cherrah, and K. Alaoui, “Radical-Scavenging Activity and Ferric Reducing Ability of *Juniperus thurifera* (L.), *J. oxycedrus* (L.), *J. phoenicea* (L.) and *Tetraclinis articulata* (L.),” *Adv Pharmacol Sci*, vol. 2016, p. 6392656, 2016.
- [56] F. Xiao, T. Xu, B. Lu, and R. Liu, “Guidelines for antioxidant assays for food components,” *Food Frontiers*, vol. 1, no. 1, p. 60–69, 2020.
- [57] N. R. Bhalodia, P. B. Nariya, R. N. Acharya, and V. J. Shukla, “In vitro antioxidant activity of hydro alcoholic extract from the fruit pulp of *Cassia fistula* Linn,” *Ayu*, vol. 34, no. 2, pp. 209–214, Apr 2013.
- [58] S. Aryal, M. K. Baniya, K. Danekhu, P. Kunwar, R. Gurung, and N. Koirala, “Total phenolic content, flavonoid content and antioxidant potential of wild vegetables from western nepal,” *Plants*, vol. 8, no. 4, p. 96, 2019.
- [59] G. Gashahun and L. Solomon, “tudy of the antioxidant activities of avocado (*persea americana* mill.) and three banana (*musa paradisiac* l.),” *Anatomy Physiol Biochem Int J*, vol. 6, no. 1, p. 100, 2019.
- [60] R. A. Khan, M. R. Khan, S. Sahreen, and M. Ahmed, “Assessment of flavonoids contents and in vitro antioxidant activity of *Launaea procumbens*,” *Chem Cent J*, vol. 6, no. 1, p. 43, May 2012.

- [61] P. Prieto, M. Pineda, and M. Aguilar, "Spectrophotometric quantitation of antioxidant capacity through the formation of a phosphomolybdenum complex: Specific application to the determination of vitamin e," *Analytical Biochemistry*, vol. 269, no. 2, p. 337–341, 1999.
- [62] F. Shariffar, G. Dehghn-Nudeh, and M. Mirtajaldini, "Major flavonoids with antioxidant activity from teucrium polium l." *Food Chemistry*, vol. 112, no. 4, p. 885–888, 2009.
- [63] C. Wan, Y. Yu, S. Zhou, W. Liu, S. Tian, and S. Cao, "Antioxidant activity and free radical-scavenging capacity of *Gynura divaricata* leaf extracts at different temperatures," *Pharmacogn Mag*, vol. 7, no. 25, pp. 40–45, Jan 2011.
- [64] C. A. Anosike, O. Obidoa, and L. U. Ezeanyika, "Membrane stabilization as a mechanism of the anti-inflammatory activity of methanol extract of garden egg (*Solanum aethiopicum*)," *Daru*, vol. 20, no. 1, p. 76, Nov 2012.
- [65] K. Gunathilake, K. Ranaweera, and H. Rupasinghe, "In vitro anti-inflammatory properties of selected green leafy vegetables," *Biomedicines*, vol. 6, no. 4, p. 107, 2018.
- [66] D. B. Aidoo, D. Konja, I. T. Henneh, and M. Ekor, "Protective Effect of Bergapten against Human Erythrocyte Hemolysis and Protein Denaturation In Vitro," *Int J Inflamm*, vol. 2021, p. 1279359, 2021.
- [67] P. Ranasinghe, P. Ranasinghe, W. P. Abeysekera, G. A. Premakumara, Y. S. Perera, P. Gurugama, and S. B. Gunatilake, "In vitro erythrocyte membrane stabilization properties of *Carica papaya* L. leaf extracts," *Pharmacognosy Res*, vol. 4, no. 4, pp. 196–202, Oct 2012.
- [68] M. A. Navarra, C. Dal Bosco, J. Serra Moreno, F. M. Vitucci, A. Paolone, and S. Panero, "Synthesis and Characterization of Cellulose-Based Hydrogels to Be Used as Gel Electrolytes," *Membranes (Basel)*, vol. 5, no. 4, pp. 810–823, Nov 2015.
- [69] S. Palantöken, K. Bethke, V. Zivanovic, G. Kalinka, J. Kneipp, and K. Rademann, "Cellulose hydrogels physically crosslinked by glycine:synthesis, characterization, thermal and mechanical properties," *Applied Polymer Science*, vol. 137, p. 48380, 2019.

- [70] H. Wang, Y. Liu, K. Cai, B. Zhang, S. Tang, W. Zhang, and W. Liu, "Antibacterial polysaccharide-based hydrogel dressing containing plant essential oil for burn wound healing," *Burns amp; Trauma*, vol. 9, 2021.
- [71] M. S. Rahman, M. M. Islam, M. S. Islam, A. Zaman, T. Ahmed, S. Biswas, S. Sharmeen, T. U. Rashid, and M. M. Rahman, "Morphological characterization of hydrogels," *Polymers and Polymeric Composites: A Reference Series*, p. 819–863, 2019.
- [72] Y. Zu, Y. Zhang, X. Zhao, C. Shan, S. Zu, K. Wang, Y. Li, and Y. Ge, "Preparation and characterization of chitosan–polyvinyl alcohol blend hydrogels for the controlled release of nano-insulin," *International Journal of Biological Macromolecules*, vol. 50, no. 1, p. 82–87, 2012.
- [73] N. Gull, S. M. Khan, M. T. Zahid Butt, S. Khalid, M. Shafiq, A. Islam, S. Asim, S. Hafeez, and R. U. Khan, "study of chitosan-based multi-responsive hydrogels as drug release vehicles: a preclinical study," *RSC Adv*, vol. 9, no. 53, pp. 31 078–31 091, Sep 2019.
- [74] M. Tanaka, G. Girard, R. Davis, A. Peuto, and N. Bignell, "Recommended table for the density of water between 0 nbsp;c and 40 nbsp;c based on recent experimental reports," *Metrologia*, vol. 38, no. 4, p. 301–309, 2001.
- [75] Z. Xia, M. Patchan, J. Maranchi, J. Elisseeff, and M. Trexler, "Determination of crosslinking density of hydrogels prepared from microcrystalline cellulose," *Journal of Applied Polymer Science*, vol. 127, no. 6, p. 4537–4541, 2012.
- [76] M. N. Alam, M. S. Islam, and L. P. Christopher, "Sustainable production of cellulose-based hydrogels with superb absorbing potential in physiological saline," *ACS Omega*, vol. 4, no. 5, p. 9419–9426, 2019.
- [77] F. Ganjil, S. Vasheghani-Farahani, and E. Vasheghani-Farahani, "Theoretical Description of Hydrogel Swelling: A review," *Iranian Polymer Journal*, vol. 19, no. 5, pp. 375–398, 2010.

- [78] Q. Chai, Y. Jiao, and X. Yu, "Hydrogels for Biomedical Applications: Their Characteristics and the Mechanisms behind Them," *Gels*, vol. 3, no. 1, Jan 2017.
- [79] P. Andrade-Vivero, E. Fernandez-Gabriel, C. Alvarez-Lorenzo, and A. Concheiro, "Improving the loading and release of NSAIDs from PHEMA hydrogels by copolymerization with functionalized monomers," *Journal of Pharmaceutical Sciences*, vol. 96, no. 4, p. 802–813, 2007.
- [80] M. K. Younis, A. Z. Tareq, and I. M. Kamal, "Optimization of swelling, drug loading and release from natural polymer hydrogels," *IOP Conference Series: Materials Science and Engineering*, vol. 454, p. 012017, 2018.
- [81] R. W. Kormsmeier and N. A. Peppas, "Solute and penetrant diffusion in swellable polymers. iii. drug release from glassy poly(hema-co-nvp) copolymers," *Journal of Controlled Release*, vol. 1, no. 2, p. 89–98, 1984.
- [82] N. S. Heredia, K. Vizuite, M. Flores-Calero, K. Pazmiño V, F. Pilaquinga, B. Kumar, and A. Debut, "Comparative statistical analysis of the release kinetics models for nanoprecipitated drug delivery systems based on poly(lactic-co-glycolic acid)," *PLoS One*, vol. 17, no. 3, p. e0264825, 2022.
- [83] N. S. Nemeş, C. Ardean, C. M. Davidescu, A. Negrea, M. Ciopec, N. Duţeanu, P. Negrea, C. Paul, D. Duda-Seiman, and D. Muntean, "Antimicrobial Activity of Cellulose Based Materials," *Polymers (Basel)*, vol. 14, no. 4, Feb 2022.
- [84] O. A. Wintola and A. J. Afolayan, "The antibacterial, phytochemicals and antioxidants evaluation of the root extracts of *Hydnora africana* Thunb. used as antidiarrheal in Eastern Cape Province, South Africa," *BMC Complement Altern Med*, vol. 15, p. 307, Sep 2015.
- [85] S. Arora, S. A. Saquib, Y. A. Algarni, M. A. Kader, I. Ahmad, M. Y. Alshahrani, P. Saluja, S. M. Baba, A. M. Abdulla, and S. S. Bavabeedu, "Synergistic Effect of Plant Extracts on Endodontic Pathogens Isolated from Teeth with Root Canal Treatment Failure: An In Vitro Study," *Antibiotics (Basel)*, vol. 10, no. 5, May 2021.

- [86] J. N. Payne, H. K. Waghvani, M. G. Connor, W. Hamilton, S. Tockstein, H. Moolani, F. Chavda, V. Badwaik, M. B. Lawrenz, and R. Dakshinamurthy, “Novel Synthesis of Kanamycin Conjugated Gold Nanoparticles with Potent Antibacterial Activity,” *Front Microbiol*, vol. 7, p. 607, 2016.